Modular Diffusion Policy Training: Decoupling and Recombining Guidance and Diffusion for Offline RL

Anonymous authors
Paper under double-blind review

Abstract

In classifier-free guidance(CFG) for offline reinforcement learning(RL), the diffusion model and its guidance are typically trained jointly and applied jointly as the policy network. Before the guidance network has converged, it provides unstable or even misleading gradient shifts for reward optimization. Such strict coupling also prevents the guidance module from being reused across different diffusion models. We propose Guidance-First Diffusion Training (GFDT), which pretrains and freezes the guidance model before diffusion policy learning. This decoupling reduces peak memory and computational overhead by 38.1%, and reduces required diffusion training steps by 65.6% and 27.66% on locomotion and navigation tasks, respectively. Beyond these efficiency gains, the method achieves significant performance improvements of up to 43.16% and 60.98% on these respective offline RL benchmarks. Moreover, we uncover a strong plug-and-play property: Cross-algorithm swaps (e.g., Implicit Q-Learning (IDQL) guidance for Diffusion Q-Learning (DQL) policies) perform comparably to the stronger of the two, despite never being co-trained.

Our theoretical analysis also demonstrates that GFDT facilitates convergence to an optimal guidance and accelerates the training process. We further prove that plug-and-play remains valid as long as the guidance and the diffusion model are trained with the same data distribution. Limitations arising from dataset mismatch are analyzed in detail, which further underscores the necessity of distributional alignment. This work opens a new line of research by treating diffusion and guidance as modular units that can be recombined, rather than as a monolithic process, suggesting a paradigm that may guide the future development of diffusion-based RL.

1 Introduction

By formulating policy learning as a conditional generative process, **diffusion policies** are capable of modeling complex, multimodal behaviors. Building on this perspective, diffusion-based policies have emerged as a powerful paradigm for behavior generation in offline decision-making. Diffusion policies for offline RL are typically composed of two core modules: a generative diffusion model that produces actions through iterative denoising, and a guidance module that provides gradient bias to steer generation toward higher-reward behavioral modes. This design is known as the **CFG** paradigm(Ho & Salimans, 2022). This guidance–diffusion paradigm has proven highly effective, achieving strong empirical success across diverse offline RL and robotic control benchmarks. Despite this success, since the guidance module and the diffusion model are trained jointly and tightly coupled in inference, TWO CHALLENGES exist: 1)Before the guidance module has converged, it cannot provide effective guidance to the diffusion model or even mislead the training process (Kim et al., 2023). 2)This tightly coupled diffusion and guidance usage prevents re-usage across different combinations of network modules.

Existing methods solve CHALLENGE 1 by pretraining the diffusion model and then letting the diffusion model generate samples for the guidance training. This pipeline overlooks data distribution shift and assumes generated samples remain unbiased. If the diffusion backbone contains modeling errors, synthetic samples replicate and amplify those biases. Furthermore, such diffusion models are trained merely to mimic the dataset's empirical distribution without reward prioritization. In this work, we take the opposite approach:

pre-training the guidance module, then freezing it to guide the diffusion model, which is called Guidance-First Diffusion Training (GFDT). This design offers four parallel advantages. 1)Because the entire model is trained solely on the dataset, without introducing synthetic samples that could contaminate the offline data. 2) As a purely offline RL formulation, the method naturally does not involve exploration, removing any ambiguity about environment sampling or online exploration requirements. 3) Unlike the existing pipelines that train the diffusion model to generate mixed-quality samples, GFDT updates diffusion using only reward-aligned gradient shifts. This converged guidance module ensures every generated action is already value-optimized rather than unconstrained. 4) Since diffusion learning is guided by a well-trained guidance signal, optimization converges substantially faster by avoiding unstable early-stage guidance updates.

To solve Challenge 2, CFG methods can be modularized: Further, we cross-combined components from models trained under different frameworks. Specifically, we took the guidance module from an IDQL model and paired it with a completely separate DQL diffusion model—one that had never been trained in conjunction with the IDQL guidance. The plug-and-play (PAP) module and its reversed model are functional, and the performance is comparable with the stronger of these two, and has a significantly better early training stage, outperforming both the baselines. This result strongly suggests that the relationship between the guidance module and the diffusion model is modular and flexible, and therefore, highlights a promising direction for future research.

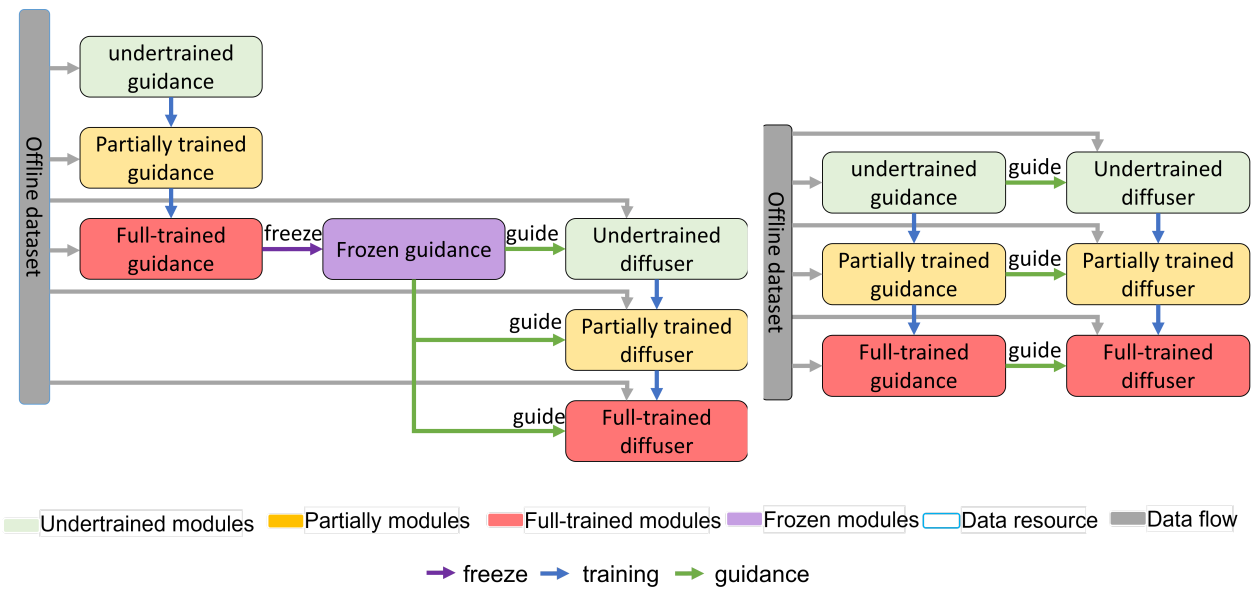

Figure 1: **Schematic Illustration of GFDT versus Traditional CFG.** GFDT (left) first trains and freezes the guidance module before diffusion training, ensuring that diffusion is guided only by a converged and reliable guidance signal. In contrast, traditional CFG (right) jointly trains guidance and diffusion, during which diffusion is influenced by immature guidance for a substantial portion of training. This figure is intended to provide intuition about training dynamics rather than to define formal modules or ablation stages. The terms “undertrained” and “partially trained” are used qualitatively and do not correspond to specific experimental regimes.

Algorithm 1 Guidance-First Diffusion Training (GDFT)

Require: Offline dataset $\mathcal{D} = \{(s, a, r, s')\}$, Q-network Q_ϕ, diffusion model ϵ_θ, guidance scale λ, training steps N_q, N_θ

// **Step 1: Train Q-function (guidance model)**
for $i = 1$ to N_q **do**
  Sample minibatch $(s, a, r, s') \sim \mathcal{D}$
  TD target: $y \leftarrow r + \gamma \cdot \max_{a'} Q_\phi(s', a')$
  Update Q_ϕ to minimize $\mathcal{L}_Q = \|Q_\phi(s, a) - y\|^2$
Freeze Q_ϕ
// **Step 2: Train diffusion model with frozen guidance**
for $j = 1$ to N_θ **do**
  Sample $(s, a_0) \sim \mathcal{D}$
  Add noise: $a_t \leftarrow \sqrt{\bar{\alpha}_t} a_0 + \sqrt{1 - \bar{\alpha}_t} \cdot \epsilon$, $\epsilon \sim \mathcal{N}(0, I)$
  Predict noise: $\hat{\epsilon} \leftarrow \epsilon_\theta(a_t, s, t)$
  Update ϵ_θ to minimize $\mathcal{L}_{\text{diff}} = \|\hat{\epsilon} - \epsilon\|^2 + \mathcal{L}_Q$
  ▷ Q_ϕ frozen; $\mathcal{L}_Q$ still updates ϵ_θ
Return trained ϵ_θ, frozen Q_ϕ

Inference:
for denoise steps **do**
  Sample candidate $a_k \sim \pi_\theta(\cdot|s)$
  Apply guidance: $a_{k-1} \leftarrow a_k + \lambda \cdot \nabla_a Q_\phi(s, a_k)$

The detailed pseudo-codes the traditional CFG, and a diagram comparison can be found in Appendix A.1. In prior works, diffusion-based policies are interpreted as actors, and Q-based guidance modules are interpreted as critics. In this paper, we use the terms Diffusion Model and Guidance Module to emphasize that our method relies on diffusion dynamics rather than generic Actor-Critic training.

2 Preliminaries

In offline RL, the objective is to learn a policy $\pi_\theta(a|s)$ that maximizes the expected return using only a fixed dataset $D = \{s, a, r, s'\}$, with interaction to the environment only at the inference stage (Levine et al., 2020). When diffusion models are used as policies, several offline RL methods—including DQL (Yang et al., 2023), Exponential Diffusion Process(EDP) (Kang et al., 2023), and IDQL (Hansen-Estruch et al., 2023)—adopt a *conditional denoising diffusion process*. The policy is defined implicitly by the reverse denoising procedure: $\hat{a}_0 \sim \pi_\theta(\cdot \mid s)$.

Q-Guided Diffusion : Q-Guided Diffusion(Janner et al., 2022) has a forward noising process and a reverse denoising process. The forward noising process gradually perturbs a clean action a_0 into a noisy version a_k:

$$a_k = \sqrt{\bar{\alpha}_k}\, a_0 + \sqrt{1 - \bar{\alpha}_k}\, \epsilon, \quad \epsilon \sim \mathcal{N}(0, I), \quad \bar{\alpha}_k = \prod_{i=1}^{k} \alpha_i,$$

where $k \in \{1, \ldots, T\}$ denotes the diffusion timestep (or noise level), and $\bar{\alpha}_k$ is the cumulative product of noise scheduling coefficients . A denoising network $\epsilon_\theta(a_k, k, s)$ is trained to recover the clean action a_0 from its noisy counterpart $a_k \sim \mathcal{N}(0, I)$. During reverse diffusion, we can form an estimate of the clean action:

$$\hat{a}_0 = \frac{1}{\sqrt{\bar{\alpha}_k}} \Big(a_k - \sqrt{1 - \bar{\alpha}_k} \cdot \epsilon_\theta(a_k, k, s) \Big). \tag{1}$$

The behavior clone loss is formulated as: $\mathcal{L}_{\text{BC}} = \mathbb{E}_{a_0, \epsilon, t}[\|\epsilon_\theta(a_t, t, s) - \epsilon\|^2]$. To incorporate reward information, Q-guided diffusion introduces an actor loss $\mathcal{L}_Q$, and the entire loss becomes: $\mathcal{L}_{\text{actor}} = \mathcal{L}_{\text{BC}} + \eta\, \mathcal{L}_Q$, which is the sum of the behavior cloning loss, and Q-loss, which is controlled by the strength of η.

Here $Q_\phi(s, a)$ denotes the learned Q-function, i.e., an estimation of the expected discounted return starting from state s and action a: $Q_\varphi(s, a) \approx \mathbb{E}[\sum_{t=0}^{\infty} \gamma r_t \Big| s_0 = s, a_0 =$

$a]$, (γ is the discount factor, r_t the reward at step t). For stable guidance, we normalize this value by its expectation over sampled actions, defining $\tilde{Q}_\phi(s,a) = Q_\phi(s,a)/\mathbb{E}_a[Q_\phi(s,a)]$. This normalization ensures scale invariance of the guidance signal and enables interchangeable use of guidance modules across actor-critic variants (e.g., DQL and IDQL) without a mismatch in magnitude.(A more detailed derivation is provided in section3.)

A similar design also exists at inference time, the Q-network provides explicit guidance by adjusting the sampled actions:

$$\tilde{a}_0 = a_0 + \lambda \frac{\nabla_a Q_\phi(s,a_0)}{\|\nabla_a Q_\phi(s,a_0)\| + \epsilon}, \tag{2}$$

where λ balances exploitation of the learned Q-function against fidelity to the diffusion. The normalizing process is inherent from (Ho et al., 2020) and is expected to be important in the modular and plug-and-play designs.

Diffusion Q-learning (DQL): The DQL model modified the traditional Q-guided diffusion and applied a variation of the Deep Q network called double Q to improve the accuracy of the Q-value estimation (**?**).

$$\mathcal{L}_\pi^{\mathrm{DQL}}(\theta) = -\mathbb{E}_{s\sim\mathcal{D}}\left[\min\left(Q_{\phi_1}(s,a^0), Q_{\phi_2}(s,a^0)\right)\right], \quad \text{where } a^0 \sim \pi_\theta(\cdot|s) \tag{3}$$

Implicit Diffusion Q-learning (IDQL). Unlike DQL, which directly incorporates the reward target into the diffusion training, IDQL adopts a two-stage design. During training, the diffusion model is updated purely via behavior cloning from the dataset, without any explicit Q-guidance. In parallel, a separate Q-value network is learned to estimate $Q(s,a)$. At inference time, the diffusion model offers candidate actions, and the guidance module evaluates them with the Q-network through a one-hot encoding scheme, and selects the action with the highest estimated Q-value. Compared to traditional Q-guided diffusion, IDQL thus applies the guidance entirely to the inference stage rather than the training stage. Although IDQL does not leverage the Q-value estimator to directly guide diffusion during training, the implementation still places the Q-network update within the same training loop as the diffusion model. This coupling is not theoretically necessary, and the consequence is a substantially higher computational and memory usage. There is a detailed analysis of the difference between IDQL and GFDT in Appendix A.2. Since IDQL does not employ diffusion guidance during training, it tends to underperform on dense-reward tasks that require fine-grained, step-wise policy optimization. In contrast, it performs well on in-distribution, goal-oriented environments such as AntMaze, which are evaluated based on task success rather than on the efficiency or smoothness of the trajectory.

Efficient Diffusion Policy (EDP) introduces a key modification on traditional Q-guided diffusion: *one-step denoising*. Instead of running the full reverse chain to generate actions, EDP corrupts a dataset action a^0 to a^k in one step, and then one-step-reconstructs an approximate clean action $\hat{a}^0$ using the denoise backward path as Equation 1 in Appendix **??**. This *action approximation* replaces expensive sampling with a lightweight inference step, making EDP orders of magnitude faster to train.

In traditional diffusion policies, generating a clean action a^0 requires running a long reverse chain:

$$a^T \to a^{T-1} \to \cdots \to a^0,$$

where T is typically large (e.g., 100–1000). This iterative procedure is computationally expensive.

Instead, EDP corrupts a dataset action a^0 directly into a noisy action a^k in one step:

$$a^k = \sqrt{\bar{\alpha}_k}\, a^0 + \sqrt{1-\bar{\alpha}_k}\, \epsilon, \quad \epsilon \sim \mathcal{N}(0,I). \tag{4}$$

Then, it reconstructs an approximate clean action $\hat{a}^0$ by applying the denoiser once:

$$\hat{a}^0 = \frac{1}{\sqrt{\bar{\alpha}_k}}\, a^k - \frac{\sqrt{1-\bar{\alpha}_k}}{\sqrt{\bar{\alpha}_k}} \cdot \epsilon_\theta(a^k, k, s), \tag{5}$$

where ϵ_θ is the learned denoising network conditioned on state s.

Role of Q-guidance Since the one-step approximation introduces bias, EDP relies more strongly on the Q-function to refine $\hat{a}^0$. In practice, the algorithm evaluates candidate actions using Q-values and adjusts them toward high-value regions, which compensates for the reduced accuracy of the denoising step.

The main differences are 1)Cost reduction: iterative sampling ($O(T)$ steps) $\rightarrow$ one-step approximation ($O(1)$). 2)Trade-off:less precise denoising $\rightarrow$ stronger dependence on Q-guidance. 3)Outcome: training time reduced by orders of magnitude (days $\rightarrow$ hours), at the expense of slightly noisier reconstructions. In summary, EDP is an acceleration of traditional CFG diffusion.

These three methods are the baselines of our methods. Currently, our modifications are typically only applied to TD-based methods and cannot be applied to Trajectory-Based methods(e.g., (Janner et al., 2022; Ajay et al., 2023)) as they use return annotations for full sequences $\tau = (s_0, a_0, ..., s_T)$. However, experiments showed low convergence rates and suboptimal precisions in their Q-value predictions, and therefore, Guidance-First Diffusion Training showed little improvement. We attribute this observation to the following factors: when the trajectory is long, the return may be noisy due to stochastic behavior policies, so reward attribution over entire sequences can be ambiguous. (It is hard to infer which action caused the reward change.) In contrast, TD-based methods that work on (s, a) pairs avoid this issue and support more granular, local learning signals. Efficient Diffusion Policy (EDP) is a variant of Q-guided diffusion that primarily improves computational efficiency. Its central idea is **one-step denoising**, which bypasses the expensive multi-step reverse process used in standard diffusion policies.

3 Methodology

Having introduced the GFDT method and modular module composition in the introduction, we now extend the discussion with a mathematical model to justify the approach. First, we explain why a pretrained, converged model can provide more accurate guidance to the diffusion model, better than an unconverged model that is trained jointly with it, thereby accelerating the training process. Second, we prove that as long as the guidance model can provide a direction that leads to reward improvement and the step size is small enough, it is sufficient for guiding the diffusion model, even if the guidance model was not co-trained with the diffusion model.

Theoretical Motivation. We build upon the theoretical framework established by Theorem (Fujimoto et al., 2019a), which introduces Batch-Constrained Q-Learning (BCQL) as a value-based method with provable convergence guarantees under offline settings. *Given a deterministic Markov Decision Process (MDP) and coherent batch $\mathcal{B}$, along with standard Robbins-Monro convergence conditions on the learning rate, BCQL converges to $Q^{\pi_{\mathcal{B}}}(s, a)$, where $\pi^*(s) = \arg\max_{a \text{ s.t. } (s,a)\in\mathcal{B}} Q^{\pi_{\mathcal{B}}}(s, a)$. This policy is guaranteed to match or outperform any behavioral policy contained in the dataset.*

Batch-Constrained Guidance via Diffusion. Inspired by this result, we adopt a *batch-constrained guidance* framework for training diffusion policies. Our key design choice is to pretrain a guidance policy (e.g., a value function $Q(s, a)$ or behavioral prior) purely on the offline dataset, then use it to guide the sampling of a diffusion policy. Theorem 1 guarantees, the training on the offline dataset converges to an optimal reward estimation policy Q(s,a).

This optimized Q(s,a) is then added to the gradient update of the training process of the diffusion:

$$\nabla_\theta \mathcal{L}_{\text{total}} = \nabla_\theta \mathcal{L}_{\text{BC}} + \eta \nabla_\theta Q(s, a), \tag{6}$$

where $\mathcal{L}_{\text{BC}}$ is a behavior cloning loss that regularizes the learned policy to stay close to the empirical distribution of $\mathcal{B}$, and η controls the strength of the guidance. Both of these two parts are learned based on the same dataset $\mathcal{B}$, so term 1 offers regularization to avoid leaving the support of the offline dataset and term 2 encourages reward optimization.

To further ensure batch-constrained optimization behavior during action generation(inference step), we modify the reverse diffusion process by injecting Qvalue gradients of the pretrained module:

$$a_{t-1} \;\leftarrow\; f_{\text{diffusion}}(a_t, \hat{a}_0, t) \;+\; \lambda \frac{\nabla_a Q(s, \hat{a}_t)}{\|\nabla_a Q(s, \hat{a}_t)\| + \varepsilon} \;+\; \sqrt{2\tau_t}\, \xi_t, \tag{7}$$

where λ is a guidance coefficient. This operation encourages the final action a_0 to lie in high-reward regions. Importantly, because the value function $Q(s, a)$ is trained on the offline dataset $\mathcal{B}$, and the diffusion model itself models the same data distribution. Intuitively, in every inference step, the diffusion model generates an action, and the Q module shifts the gradient in a magnitude that is smaller than or equal to λ. So, the generated action must be inside the region of the dataset $\mathcal{B}$. Adding the small gradient shift, the entire action is still inside or close to the dataset $\mathcal{B}$'s coverage. Thus, the value-aware perturbation can be interpreted as a form of approximate, soft batch-constrained policy improvement. For a more detailed explanation, please check Appendix D

On the contrary, before sufficient training, the inaccurate gradient will misshape the diffusion distribution and prolong the training process by adding incorrect information to the optimization, which may or may not be corrected in later training.

Admittedly, our approach does not strictly satisfy all assumptions of BCQL: the network may converge not to the true Bellman optimum but to a local minimum, an inherent limitation of non-convex optimization that cannot be fully avoided. However, we inherit its core principle: The guidance can be trained to an optimal value estimator, and any value-based guidance must be constrained to the data distribution to guarantee that the gradient guidance is reliable. This proof is also consistent with the experiment results (Section 4): in distribution guidance improves the performance of the CFG. Validated by inverse reasoning, the application scope of the GFDT method in Section 5 showed that out-of-distribution guidance cannot guarantee efficient guidance, and in practice, often jeopardizes the performance.

Theorem 2: *Joint training of the guidance module and the diffusion policy is not required. A pretrained Q-network Q_ϕ can be modularized and directly applied to guide the diffusion model, as long as Q_ϕ accurately estimates state-action values within the dataset support $\mathcal{B}$.*

We consider the perturbed diffusion sampling process after the action generation:

$$a_t = a_t + \lambda \cdot \frac{\nabla_a Q_\phi(a_t)}{\|\nabla_a Q_\phi(a_t)\|} + \sqrt{2\tau_t}\,\xi_t, \tag{8}$$

where λ is a small step size and τ_t controls the annealed noise. The gradient $\nabla_a Q_\phi$ provides a reward-sensitive vector field over the action space.

Directional Alignment and Convergence. As long as the value gradient is directionally positive correlation the diffusion model's score function(i.e., $\cos\langle \nabla Q_\phi, \nabla \log p(a)\rangle > 0$), then the expected change in Q_ϕ over one step is

$$\mathbb{E}[Q_\phi(a_{t+1}) - Q_\phi(a_t)] \approx \lambda \cdot \cos\theta_t \cdot \|\nabla Q_\phi(a_t)\| + \mathcal{O}(\sqrt{\tau_t}). \tag{9}$$

Moreover, since the noise is Gaussian, we have: $\lim_{T\to\infty} \frac{1}{T}\sum_{t=1}^{T} \xi_t = 0$ (in expectation), meaning the cumulative effect of noise diminishes over time, and the value gradient dominates in expectation. The action will be guided towards a rewarding-increasing direction gradually.

A pretrained Q-function can reliably steer the diffusion process toward high-reward regions without destabilizing sampling, as long as the step size is small and the guidance remains positively beneficial and smooth. This justifies the plug-and-play design of our framework and aligns with the batch-constrained principle in offline RL.

Heuristic sample-complexity argument. To connect our theoretical discussion to practical training savings, we provide a heuristic estimate of how many gradient steps can be saved. A standard result in nonparametric estimation theory states that estimating the gradient of a smooth function from N i.i.d. samples achieves an error that decays as $O(1/\sqrt{N})$ (Wasserman, 2006; Stone, 1982). For a Lipschitz function class with constant L, a guidance model Q_ϕ trained to accuracy on dataset $\mathcal{B}$, the gradient estimation error satisfies:

$$\mathbb{E}\|\nabla_a Q_\phi - \nabla_a Q^*\| \le C * \frac{L}{\sqrt{N}} + \epsilon \tag{10}$$

Table 1: The parameters used in Equation (10)

$\nabla_a Q_\phi$	Pretrained Guidance Gradient	ϵ	Final training error of Q_ϕ
L	Lipschitz constant of the Q-function class	N	Number of samples in dataset $\mathcal{B}$
$\nabla_a Q^*$	True gradient of the optimal Q-function	C	a constant depends on the underlying function class

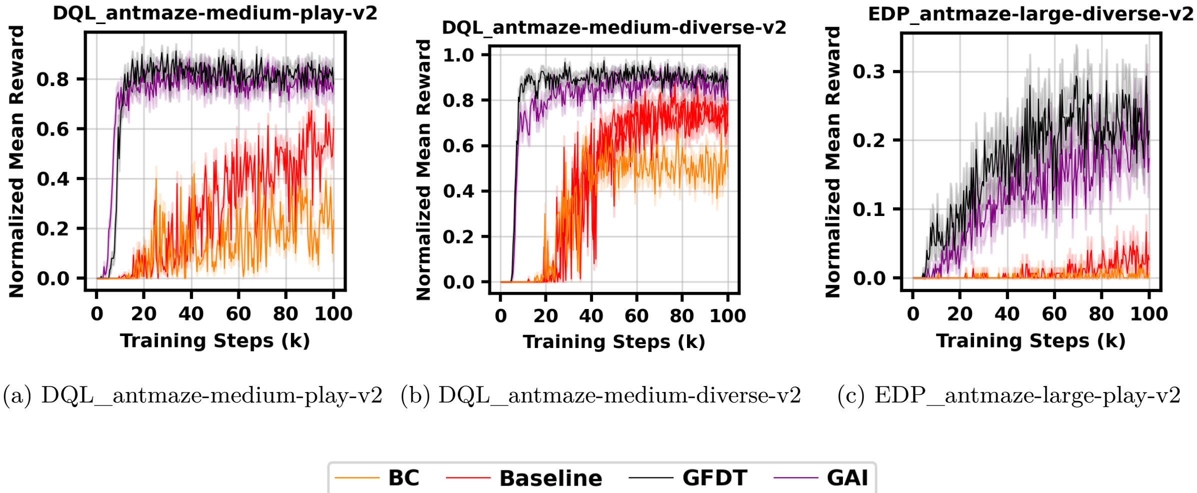

(a) DQL_antmaze-medium-play-v2 (b) DQL_antmaze-medium-diverse-v2 (c) EDP_antmaze-large-play-v2

Figure 2: **Training performance of proposed algorithms on benchmarks.**

Heuristically, although in RL practice the Lipschitz constant L is rarely specified, in related areas (e.g., WGAN with spectral normalization (Miyato et al., 2018)) one often enforces $L = 1$. Under this convention, Eq (10) implies that achieving a guidance accuracy of $\mathbb{E}\|\nabla_a Q_\phi - \nabla_a Q^*\| = 0.01$ would require about $N = 1/\mathbb{E}\|\nabla_a Q_\phi - \nabla_a Q^*\|^2 = 10^4$ effective samples (equivalently, $\sim 10^4$ gradient updates of the Q network). In more parameter-sensitive scenarios, pushing the accuracy further to $\mathbb{E}\|\nabla_a Q_\phi - \nabla_a Q^*\| = 0.001$ would require as many as $N = 10^6$ effective samples (i.e., 10^6 gradient updates). This illustrates the significant optimization steps that are potentially misguided before the guidance converges, and shows how our method helps reduce otherwise wasted early training of the diffusion model. Pretraining is therefore essential to ensure that guidance has semantic meaning before being applied in generation Appendix. I.

4 Experiments

We evaluate our method on standard tasks from the PyBullet D4RL benchmark (Fu et al., 2021; Foundation, 2024). To ensure fair comparison, we re-train three seeds of three representative diffusion-based offline RL algorithms—EDP, DQL, and IDQL(module interchange)—based on the dataset and benchmark code from (Wang et al., 2024). These methods serve as illustrative examples of our theory, which can be easily extended to more diffusion methods. For more details about the environment setting, please check Appendix C. The detail comparison between our model and the baseline models is shown in Appendix E.

4.1 Performance of GFDT

All experiments were conducted using PyTorch on a high-performance computing (HPC) cluster. We adhered to any assigned framework for our work because the focus of this paper is not restricted to any specific computational framework.

From the Table 10 and Table 11, in the environments and algorithms, GFDT outperformed baseline models in 11/12 environments for DQL and 8/12 environments for EDP. More importantly, the early performance of the GFDT is significantly better than the baseline model as shown in Table 5. On MuJoCo tasks, our method achieves an average improvement of about 2.9%, while on AntMaze tasks, the improvement ranges from 14% to 20%. This indicates that the proposed method brings consistent yet moderate gains on dense-reward locomotion tasks, and substantially larger benefits on sparse-reward, goal-directed environments.The improve of the DQL model is higher than the EDP model. Formally, DQL can be abstracted as $x_t = f(x_{t+1}, \text{guidance}_t)$ where each step depends on both the previous state x_t and a step-wise guidance signal, leading to an iterative accumulation of guidance effects. In contrast, EDP follows a single-step mapping $x_0 = f(x_T, \text{guidance})$,

Table 2: Comparison with standard offline RL baselines on D4RL tasks. Results ReBR, short for REBRAC from (Wu et al., 2019) DICE (Ma et al., 2024), CQL are taken from (Kumar et al., 2020), IQL from (Kostrikov et al., 2022), EDP-GFDT and DQL-GFDT, DGID and IGDD are ours. (These abbreviations are in the Appendix. **??**)

Env	ReBR	DICE	CQL	IQL	DQL_GFDT	EDP_GFDT	DGID	IGDD
HCME	101.1±1.5	97.3±0.6	45.3±0.3	92.7±2.8	90.2±0.4	87.2±0.0	85.61±0.01	84.77±0.00
HCMR	51.0±0.2	49.2±0.9	45.3±0.3	42.1±3.6	**67.9±0.3**	**64.4±0.0**	**70.6±0.8**	**69.8±0.0**
HCMV	65.6±1.0	60.0±0.6	46.9±0.4	50.0±0.2	**67.0±0.6**	59.3±0.4	60.9±0.9	60.9±0.2
HOME	107.0±6.4	112.2±0.3	96.6±2.6	85.5±29.7	**172.3±1.1**	**163.9±0.0**	**182.4±0.0**	**182.7±0.0**
HOMR	98.1±1.6	102.3±2.1	89.6±13.2	89.6±13.2	**153.0±0.8**	**146.4±1.7**	**157.2±0.0**	**157.2±0.0**
HOMV	102.0±1.0	100.2±3.2	61.9±6.4	65.2±4.2	**147.0±1.1**	**141.6±0.0**	**136.5±0.2**	**136.5±0.2**
WAME	111.6±0.3	114.1±0.5	104.6±1.1	112.1±0.5	**117.6±0.3**	**116.6±0.0**	**118.1±0.0**	**118.4±0.0**
WAMR	77.3±7.9	90.8±2.6	76.8±1.0	75.4±9.3	**95.6±4.8**	83.8±0.4	**93.1±0.94**	87.5±0.7
WAMV	82.5±3.6	89.3±1.3	79.5±3.2	80.7±3.4	**87.9±0.3**	84.2±0.0	87.11±0.07	87.1±0.0
L-div	54.4±25.1	91.3±3.1	14.9	27.6±7.8	90.7±5.4	31.3±6.9	33.3±6.9	46.7±7.0
L-play	60.4±26.1	85.7±4.8	15.8	42.5±6.5	**89.3±5.6**	22.7±6.7	28.0±6.7	59.3±7.0
M-div	76.3±13.5	68.6±8.6	53.7	61.7±6.1	**97.3±4.0**	52.0±7.7	58.0±7.0	68.0±6.8
M-play	84.0±4.2	72.0±6.5	61.2	64.6±4.9	**91.3±5.3**	**118.0±10.4**	56.7±7.0	74.7±6.6

Note 1 While the algorithms were proposed in the aforementioned papers, the authors did not release their raw experimental results;all numerical values for standard baselines in Table 2 are taken from (Ma et al., 2023). These methods are considered as the strongest methods in offline RL.

Note 2 The left four columns show results from other methods, while the right four columns present results from our proposed method. The highest values in the left four columns are highlighted in blue. If a value in our method (right columns) exceeds the highest value on the left, it is shown in bold with a gray background.

Table 3: Performance comparison across tasks (DQL)

Environment	Baseline	GFDT	GAI	BC	Unfreeze
halfcheetah-expert	88.21 ± 0.28	90.43 ± 0.26	68.49 ± 1.55	85.82 ± 2.24	89.50 ± 0.23
halfcheetah-medium-expert	88.28 ± 0.53	90.18 ± 0.38	89.73 ± 0.43	85.53 ± 1.34	89.76 ± 0.61
halfcheetah-medium-replay	67.38 ± 0.34	67.93 ± 0.33	67.76 ± 0.52	55.87 ± 5.23	67.43 ± 0.37
halfcheetah-medium	59.88 ± 5.40	66.99 ± 0.60	53.36 ± 1.43	54.57 ± 4.27	55.04 ± 2.27
hopper-expert	166.76 ± 0.58	172.90 ± 0.56	162.68 ± 1.21	165.11 ± 0.67	155.15 ± 44.68
hopper-medium-expert	168.00 ± 1.18	172.31 ± 1.09	166.28 ± 1.03	166.88 ± 1.33	159.10 ± 31.75
hopper-medium-replay	151.59 ± 0.57	152.98 ± 0.75	121.97 ± 49.30	113.30 ± 35.20	150.50 ± 3.44
hopper-medium	143.92 ± 1.05	147.06 ± 1.09	71.09 ± 35.69	118.08 ± 15.41	144.59 ± 1.09
walker2d-expert	117.25 ± 0.46	120.25 ± 0.60	119.91 ± 0.52	108.05 ± 28.27	117.92 ± 0.47
walker2d-medium-expert	117.73 ± 0.35	117.63 ± 0.34	115.08 ± 1.32	117.45 ± 0.68	118.50 ± 0.73
walker2d-medium-replay	92.96 ± 0.60	95.62 ± 4.78	80.32 ± 19.52	87.14 ± 1.87	95.62 ± 4.78
walker2d-medium	87.65 ± 0.40	87.89 ± 0.27	77.33 ± 13.13	82.28 ± 0.70	87.89 ± 0.43
Average	112.47 ± 0.98	115.18 ± 0.92	99.50 ± 10.47	103.34 ± 8.10	110.92 ± 7.57
antmaze-large-diverse-v2	63.33 ± 48.19	90.67 ± 5.39	86.67 ± 5.83	66.00 ± 6.88	86.67 ± 5.83
antmaze-large-play-v2	90.00 ± 30.00	89.33 ± 5.56	88.67 ± 5.63	50.67 ± 7.07	91.33 ± 5.30
antmaze-medium-diverse-v2	93.33 ± 24.94	97.33 ± 4.01	94.00 ± 4.87	78.00 ± 6.44	96.00 ± 4.43
antmaze-medium-play-v2	67.33 ± 46.90	91.33 ± 5.30	88.67 ± 5.63	68.00 ± 6.83	93.33 ± 4.99
Average	78.50 ± 37.51	92.17 ± 5.07	89.50 ± 5.49	65.67 ± 6.80	91.83 ± 5.14

where the guidance is injected only once without iterative updates, which naturally limits its overall influence.

Table 4: Performance comparison across tasks (EDP)

Environment	EDP_baseline	GFDT	GAI	BC	Unfreeze
halfcheetah-expert	86.55 ± 0.00	86.82 ± 0.00	78.78 ± 0.52	85.82 ± 2.24	85.98 ± 0.00
halfcheetah-medium-expert	86.74 ± 0.00	87.16 ± 0.00	78.18 ± 0.15	85.53 ± 1.34	86.85 ± 0.01
halfcheetah-medium-replay	65.78 ± 0.03	64.42 ± 0.03	47.08 ± 1.90	55.87 ± 5.23	64.42 ± 0.03
halfcheetah-medium	54.59 ± 0.04	59.26 ± 0.39	53.56 ± 0.02	54.57 ± 4.27	55.33 ± 0.11
hopper-expert	161.23 ± 0.02	163.65 ± 0.02	151.93 ± 3.23	165.11 ± 0.67	162.24 ± 0.01
hopper-medium-expert	161.36 ± 0.02	163.95 ± 0.01	141.07 ± 10.51	166.88 ± 1.33	163.68 ± 0.01
hopper-medium-replay	112.16 ± 2.83	139.75 ± 6.69	114.32 ± 3.26	113.30 ± 35.20	119.91 ± 11.62
hopper-medium	141.16 ± 0.02	141.64 ± 0.01	83.25 ± 6.63	118.08 ± 15.41	141.54 ± 0.05
walker2d-expert	116.14 ± 0.00	116.34 ± 0.00	114.27 ± 0.01	108.05 ± 28.27	116.36 ± 0.00
walker2d-medium-expert	116.31 ± 0.01	116.59 ± 0.00	109.55 ± 3.05	117.45 ± 0.68	117.07 ± 0.00
walker2d-medium-replay	85.02 ± 0.01	83.77 ± 0.37	68.84 ± 3.45	87.14 ± 1.87	85.19 ± 0.02
walker2d-medium	84.24 ± 0.00	84.21 ± 0.00	58.21 ± 5.29	82.28 ± 0.70	84.44 ± 0.00
Average	105.94 ± 0.25	108.96 ± 0.63	91.59 ± 3.17	103.34 ± 8.10	106.92 ± 0.99
antmaze-large-diverse-v2	30.67 ± 6.99	31.33 ± 6.91	28.67 ± 46.67	10.67 ± 5.56	47.33 ± 7.25
antmaze-large-play-v2	21.33 ± 6.40	22.67 ± 6.70	18.67 ± 40.64	18.67 ± 6.24	25.33 ± 6.82
antmaze-medium-diverse-v2	67.33 ± 9.06	52.00 ± 7.72	2.00 ± 14.00	18.00 ± 6.46	13.33 ± 6.14
antmaze-medium-play-v2	73.30 ± 10.34	118.00 ± 10.35	90.00 ± 95.74	76.00 ± 9.28	113.33 ± 9.89
Average	48.16 ± 8.20	56.00 ± 7.92	34.83 ± 49.26	30.83 ± 6.89	49.83 ± 7.52

Table 5: Training gradient steps to get 95% performance and parameter statistics summary (batch size 256)

Env	DQL	GFDT_DQL	EDP	GFDT_EDP	DDIG	IDDG
HCEX	7600	2800 (36.84%)	18000	3600 (20.00%)	13200 (63.46%)	10400 (50.00%)
HCME	16400	2800 (17.07%)	31200	6000 (19.23%)	26400 (81.48%)	14400 (44.44%)
HCMR	8000	3200 (40.00%)	20400	8400 (41.18%)	7200 (26.47%)	35600 (130.90%)
HCM	52000	7600 (14.62%)	10800	10000 (92.59%)	6400 (7.24%)	45600 (51.60%)
HOEX	30800	15200 (49.35%)	8400	8400 (100.00%)	38400 (118.52%)	4400 (13.60%)
HOME	41600	23600 (56.73%)	24000	16800 (70.00%)	44400 (105.71%)	56000 (133.30%)
HOMR	24800	3200 (12.90%)	40800	52800 (129.41%)	71200 (127.14%)	35600 (63.60%)
HOM	79200	12800 (16.16%)	50400	76800 (152.38%)	90800 (76.95%)	19200 (16.30%)
WAEX	59600	14000 (23.49%)	10800	7200 (66.67%)	51200 (69.57%)	30400 (41.30%)
WAME	96000	72400 (75.42%)	21600	18000 (83.33%)	47600 (42.65%)	31600 (28.30%)
WAMR	26000	9600 (36.92%)	38400	10800 (28.13%)	10800 (16.07%)	400 (0.60%)
WAM	10800	3600 (33.33%)	79200	51600 (65.15%)	24000 (55.05%)	60400 (138.50%)
AVG	37733	14233 (34.40%)	29500	22533 (72.34%)	35967 (65.86%)	28667 (59.37%)
Ldiv	500000	47600 (9.52%)	1600000	900000 (56.25%)	64800 (12.96%)	400000 (80.00%)
Lplay	1300000	29200 (2.25%)	1300000	87600 (6.74%)	76400 (5.88%)	70800 (5.45%)
Mdiv	1500000	18000 (1.20%)	800000	17200 (2.15%)	37600 (2.51%)	44400 (2.96%)
Mplay	89600	15200 (16.96%)	1400000	1400000 (100.00%)	85200 (95.09%)	43200 (48.21%)
AVG	847400	27500 (7.48%)	1275000	601200 (41.28%)	66000 (29.11%)	139600 (34.16%)

4.1.1 The role of the guidance module

To analyze the role of reward guidance and whether the guidance is removable or replaceable, we conducted an ablation study of a series of training sessions. In this experiment, we compare the performance of GFDT, baseline models, an ablation study that removed the reward guidance part of the baseline training—behavior clone(BC), an ablation study on a behavior clone training with a guidance at the inference stage(GAI), an ablation study that pretrained the guidance module but did not freeze it in diffusion training.

-Beyond the superior performance of our proposed algorithm, we further investigate its other properties through the ablation Study. The pretrained but non-frozen guidance model in diffusion training outperforms the baseline but does not surpass GFDT, confirming that additional training of the guidance model is

Table 6: Parameter statistics summary for different model widths. (This model has a hidden layer size of 256.)

	128	**256**	**512**
Diffusion Params	172,230 (70.0%)	174,534 (38.1%)	172,230 (13.7%)
Guidance Params	73,986 (30.0%)	283,650 (61.9%)	1,082,370 (86.3%)
Total Memory	0.94 MB	1.75 MB	4.79 MB

unnecessary. The slight performance drop is likely caused by overfitting of the guidance model under over-training. GAI, removing the guidance module, results (in training) got worse performance and higher variance, underscoring the important role of guidance. Finally, we also tested that random guidance leads to complete failure of the diffusion model, highlighting that inaccurate guidance signals can be detrimental. This supports our claim that a valid guidance model is critical for successful training.

The training time of the diffusion model decreased significantly as shown in Table.5 with decreased computational resources—while they have the same training for the guidance module, the training steps for the diffusion module was significantly decreased. The following sections discuss how to plug and play a pretrained module into the diffusion model, making the modules reusable.

In Table 6, we analyze the number of parameters in the guidance module and the diffusion model. The parameter counts objectively reflect the memory footprint and computational cost of each component. Since we pre-train the guidance module, the peak memory usage during GFDT training only needs to accommodate the largest of these components. Therefore, we consider the effective reduction to be determined by the smaller of the two overlapping components, which corresponds to a 38.1% decrease for our model.

4.2 Plug-and-Play Model Composition

Our research reveals that diffusion models exhibit unique plug-and-play compatibility with their guidance modules, following the theoretical proof. We evaluate two hybrid configurations without any additional training: 1) DQL-as-Guidance + IDQL-as-Diffusion(IDDG), 2) IDQL-as-Guidance + DQL-as-Diffusion(DDIG). as shown in Figure 3, both combinations: (1) achieve final performance comparable to the DQL baseline, the higher one of these two models in Mujoco environments. (2)They performed lower results in Antmaze environments because the Plug and Play method does not match with the Max Q algorithm that is applied in Antmaze environments (3) They exhibited significant faster initial convergence speeds compared to baselines, and (4) maintain stability despite architectural misplacement. The detailed analysis of this ablation study is in the Appendix.F. The key point is that for environments with dense reward (Mujoco), the discrepancy or mismatch can be compensated and corrected immediately, the module interchange is applicable, and even beneficial for optimality and for smoothing the adjustments. However, for sparse rewarding environments(Antmaze) that need high precision, the error can accumulate, and the reward estimation becomes out-of-distribution, because of the mismatch.

Most importantly, despite the absence of joint training or any task-specific fine-tuning, the plug-and-play configurations achieve performance comparable to established baselines such as CQL and IQL. Although their results are slightly below the best-performing methods (e.g., DICE), the fact that two independently trained modules can be directly combined to reach this level of performance highlights the strong modular compatibility and generalization potential of our framework. This result implies that: Guidance modules can provide effective policy improvement signals regardless of diffusion model architecture with proper setup. It implies that the normalizing step in the training and inference parts is expected to be an important reason why these two modules are interchangeable, as explained in the Methodology Section Theorem 2. Finally, early-stage advantages suggest that when the modules are both under-trained and are not perfect, a differently structured model is not only unharmful, but can cross-correct with the errors of each module. We find that a guidance module—trained independently and even with a completely different architecture—can be directly applied to a diffusion model. This experiment is consistent with our theoretical analysis that, as long as the guidance model provides a reliable estimate of the reward(gradient estimate per se), it can be reused across structurally dissimilar models. Such modularity enables flexible training pipelines and paves the way for reusable, task-agnostic RL components. Finally, as we have mentioned in the theoretical part, if the guidance model is not independent trained on the same data distribution, there is no guarantee that the independent

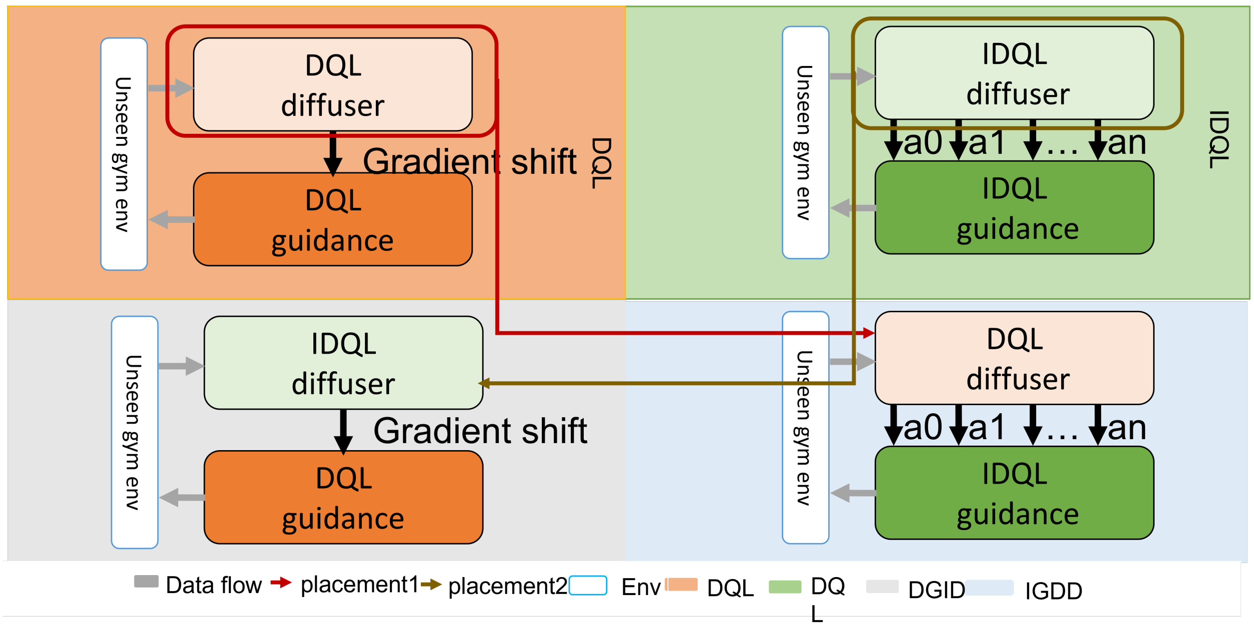

Figure 3: Diagram of plug-and-play modular configuration

module will be beneficial. In the following section, we illustrate that pretraining on out-of-distribution(OOD) data is more likely to be detrimental than beneficial in practice.

Table 7: Performance comparison with standard deviation in ± format (2 decimal places)

Dataset	**DQL**	**IDQL**	DGID	IGDD
halfcheetah-expert	88.21±0.28	71.07±0.02	85.59±6.92	81.64±0.86
halfcheetah-medium-expert	88.28±0.53	72.03±0.01	85.61±0.01	84.77±0.00
halfcheetah-medium-replay	67.38±0.34	55.90±0.00	70.58±0.84	69.79±0.01
halfcheetah-medium	59.88±5.40	52.70±0.00	60.87±0.89	60.87±0.23
hopper-expert	166.76±0.58	160.53±0.00	159.18±4.11	208.67±0.02
hopper-medium-expert	168.00±1.18	128.25±2.82	182.47±0.03	182.68±0.02
hopper-medium-replay	151.59±0.57	55.53±0.84	157.24±0.00	157.24±0.00
hopper-medium	143.92±1.05	65.94±0.26	136.53±0.23	136.53±0.20
walker2d-expert	117.25±0.46	113.78±0.00	116.64±0.14	116.64±0.02
walker2d-medium-expert	117.73±0.35	70.79±0.02	118.11±0.00	118.39±0.00
walker2d-medium-replay	92.96±0.60	71.83±0.05	93.10±0.94	87.35±0.07
walker2d-medium	87.65±0.40	66.78±0.01	87.11±0.07	87.11±0.01
Subset Avg	112.47±0.98	82.09±0.34	112.75±1.18	115.97±0.12
large-diverse	51.33±7.07	53.33±7.16	33.33±6.87	46.67±7.06
large-play	90.00±5.48	62.00±7.79	28.00±6.70	59.33±7.01
medium-diverse	93.33±4.99	82.67±7.98	58.00±7.03	68.00±6.83
medium-play	67.33±6.85	56.00±6.58	56.67±7.04	74.67±6.59
Full Avg	75.50±6.10	63.50±7.38	44.00±6.91	62.17±6.87

Table 8: Default DQl with Different Guidance Strengths Experimental Results for Expert Adroit

	relocate		pen		hammer		door	
	mean	std	mean	std	mean	std	mean	std
η=0(BC)	105.9296	±0.843	144.8144	±5.58	129.2588	±1.261	105.9296	±0.843
η=0.05	105.4705	±0.906	141.9434	±6.13	128.5337	±1.273	105.4705	±0.906
η=0.1	105.6861	±1.049	130.3630	±7.05	129.2724	±1.091	105.6861	±1.049
η=1	-0.2692	±0.2	36.6698	±7.8345	0.1452	±2.2361	-0.1484	±1.4142

5 Application scope and Limitations

To illustrate the distribution shift between datasets, We performed PCA analysis on the datasets and plotted the region that contains 60% of the data points to eliminate the instability caused by outliers. The highlighted points are the top 100 highest-reward points. The positions of these high-reward points varied significantly across datasets, even within the same environment and the shifting trade suggests the gradual converging process. The differences in the plot imply that for any given dataset, the data from another expertise level often lies in an OOD region, as shown in Table.4. The dataset distributions of other environments are show in Appendix G. Based on this observation, we conducted OOD experiments by training a guidance network on one dataset, freezing it, and then using it to guide the training of a main diffusion model on a different dataset. Across 36 tested models, 28/36(78%) exhibited significant performance degradation. Among the eight cases with good performance, half benefited from guidance modules pretrained using medium replay models, which cover a broader range of data and thus generalize better than other datasets.

From these results, we conclude that the decouple method is highly sensitive to distribution shift. Training a guidance network on in-distribution data is critical for success. Otherwise, even expert-level data cannot reliably guide training on a different distribution. This ablation study is consistent with the conclusion in the Methodology part that OOD pretraining cannot guarantee performance improvement.

Another kind of limitation of Q-guided diffusion, not only in our methods but also, is whether the guidance should exist in the training. As shown in Table 8, for high-dimensional tasks with narrow data coverage (e.g., Adroit), even slight guidance can push the policy out-of-distribution, causing performance to drop significantly. In these cases, relying solely on behavioral cloning proves more stable and effective. Conversely, for tasks with moderate difficulty and abundant data, Q-guidance can successfully enhance performance.

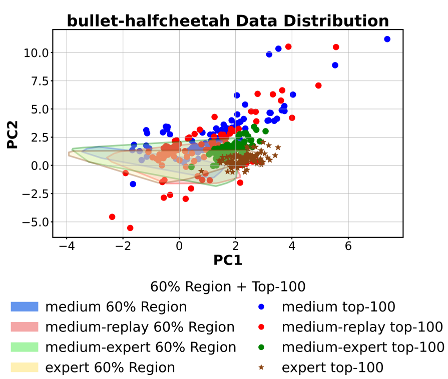

(a) Data distribution

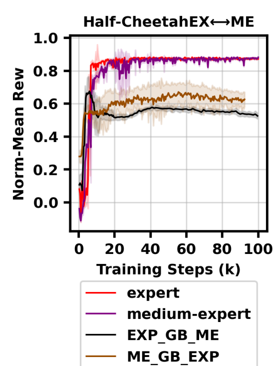

(b) Cross experiment expert & median Expert

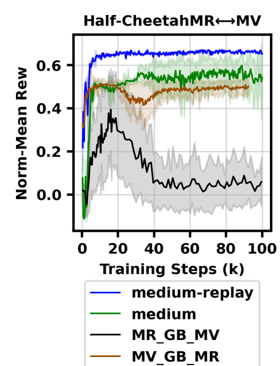

Figure 4: Cross-training of different data levels

6 Related Work

Modular and Decoupled Training: Modular training has long been pursued as a desirable paradigm. In the context of diffusion models, the earliest attempts at modularity can be traced to classifier guidance (Dhariwal & Nichol, 2021), where a pretrained diffusion model was paired with a separately trained classifier to steer sampling. This approach was unstably designed to amplify the possibility of one class while suppressing all others, ignoring that features are often shared across categories, leading to distorted and fragile guidance. Recently, energy-based guidance (Lu et al., 2023) was proposed, where a diffusion model is trained first and an energy model is subsequently learned to provide guidance. However, such post-hoc modularization has proven fragile in practice—e.g., in our own experiments, more than half of the runs diverged. In contrast, our method inverts this order: we first train a guidance module using supervised learning from offline data, and then use this frozen module to learn a diffusion. It serves as a general-purpose enhancement to existing architectures of CFG. Another line of research is semi-modularized: although IQL can be seen as a modular paradigm—learning Q-values first and then selecting one-hot action in the inference stage—it does not apply guidance during training, and its performance often lags behind joint methods such as DQL. The importance of stability under distributional shift has been repeatably mention in classic offline RL algorithms such as BCQ (Fujimoto et al., 2019b), CQL (Kumar et al., 2020), and BRAC (Wu et al., 2019), our work proposes a guidance-first modular framework that enhances training in offline RL can also be considered as a batch-constrained or conservative regularization, using the pretrained guidance to regularize diffusion process. Finally, modular training is valid, as on vision or text diffusion-based generation widely exists; large language models and vision language models have Retrieval Augmented Generations or other special models separately trained as building blocks; however, since these modules use the web-harvested data, the limitations of OOD are not well-discussed. Offline RL must contend with severe out-of-distribution issues, making modularization brittle. This challenge has been extensively studied, with methods such as BRAC (Wu et al., 2019), CQL (Kumar et al., 2020), MOPO (Yu et al., 2020), and AWAC (Nair et al., 2020) proposing different strategies to mitigate extrapolation error. Our study provides the first systematic examination of when modular guidance is feasible and demonstrates that, under the challenges of offline RL, modular training can succeed if designed around guidance-first principles.

Plug-and-Play Modular Composition. The idea of plug-and-play composability is to treat pretrained modules—originally developed for other purposes—as reusable building blocks. Such composability is rarely studied and highly empirical. We propose that plug-and-play composition requires distributional alignment. For instance, in diffusion models, CLIP-based guidance (Nichol et al., 2021; Ramesh et al., 2021) applied a pretrained vision–language model as guidance, but fails on noisy intermediate states, where distribution mismatch undermines compositionality. Circumventions exist: some prior works explore modular policy composition (Andreas et al., 2017; Peng et al., 2019), focusing on skill chaining or subpolicy selection. These methods apply the plug-ins as subproblem solvers in heuristic models instead of direct reward guidance. A common challenge concerns **I/O calibration** between modules' signal magnitude. This issue is acute in systems with complex plug-in connections, such as adapter-based methods (Mou et al., 2023; Zhang et al., 2023; Ye et al., 2023), which rely heavily on the backbone's feature space. When transferred across architectures (e.g., from SD1.5 to SDXL), their performance collapses due to representational mismatch, showing these adapters are not universal interfaces. The same logic applies in NLP, where Retrieval-Augmented Generation (RAG) (Lewis et al., 2020) often suffers when the retriever is misaligned. Related retrieval-augmented frameworks such as REALM (Guu et al., 2020), FiD (Izacard & Grave, 2021), and Atlas (Izacard et al., 2022) further highlight the need for careful design of retriever–generator alignment. Overall, the design of plug-and-play models requires careful consideration to ensure alignment and stability.

Finally, plug-and-play can be beneficial if properly implemented. Value-based RL methods often suffer from intrinsic bias, since a single network trained on limited data can easily over- or under-estimate values in unseen regions. A classical remedy is *Double Q-learning* (van Hasselt, 2010; van Hasselt et al., 2016), which decouples action selection and evaluation using two networks. Our work follows this family of ideas: inspired by Double Q-learning and ensemble learning, we leverage two independently initialized modules to cancel stochastic biases inherent in a single model, a technique widely adopted in RL but underexplored in diffusion-based policies.

Relation to Inference-Time Alignment. Inference-time alignment for diffusion models as policies, enabling controllable generation without retraining the generator (Uehara et al., 2025). They are typically formalized using ordinary, partial, or stochastic differential equations describing diffusion sampling dynamics (Dhariwal & Nichol, 2021). Model-agnostic methods exploit diffusion stochasticity through restarts, ensemble aggregation, or noise search as inference-time compute scaling (Li et al., 2023; Ma et al., 2025). Model-specific approaches formulate alignment as sampling from reward-tilted distributions modifying the original diffusion objective (Uehara et al., 2025). Among Model-specific methods, Gradient-based methods inject reward, value, or classifier gradients into denoising dynamics, including classifier and classifier-free guidance (Dhariwal & Nichol, 2021; Chung et al., 2023). Such methods require strong alignment between guidance models and diffusion policies, and remain underexplored in offline reinforcement learning (Yang et al., 2023). Our work contributes is closest to this direction, but also has fundamental difference from it. Derivative-free approaches instead post-process generated samples using candidate selection, importance sampling, or sequential Monte Carlo resampling (Ramesh et al., 2022; Zhang et al., 2024). Bayesian SMC methods rely on Feynman–Kac formulations, emphasizing posterior correction through weighting rather than stable policy learning (Skreta et al., 2025; Doucet et al., 2009).

Our work is orthogonal to the research on inference-time alignment, which focuses on goal-oriented post-processing, such as selection or resampling, applied to a fixed, pre-trained model. Instead, we modify the training and composition of the model itself: we reorder the training pipeline via Guidance-First Diffusion Training (GFDT) to ensure guidance convergence. We also demonstrate that independently trained guidance and diffusion modules can be recombined at inference time without performance degradation. This modular training perspective reveals a form of compositional flexibility that is not captured by existing inference-time alignment frameworks, and it provides a practical pathway for reusing and recombining reinforcement learning policy components across algorithms.

7 Future work

In practice, we observe that during the early stage of training, the reconstruction loss overwhelmingly dominates the overall objective, effectively outnumbering the guidance loss. As a result, for roughly the first twenty thousand gradient steps, the model primarily focuses on reconstruction, and the influence of guidance remains negligible. Once the reconstruction error has sufficiently decreased, the effect of guidance becomes more visible—its gradients start shaping the diffusion behavior toward higher-reward regions.

However, we also notice that in some cases, both in the baselines and in GFDT, applying a guidance signal can lead to unstable training behavior, occasionally causing a failed training performance collapse after initial improvement. The inverse V shape curve in Fig.4 is a good example when the guidance is not applied properly. However, OOD guidance issue is not intrinsic, but occasional failing can be fixed. A simple and effective remedy is to gradually introduce the guidance term—for example, linearly increasing its weight after the first few thousand training steps and finally applying the full weight to the model—which empirically stabilizes training and consistently prevents such failures. In our experiments, after applying this trick, training failure has never occurred.

Reproducibility and Ethics Statement

Experiments use three random seeds; hyperparameters are in Appendix C. Code, pretrained models, and scripts are available at `https://github.com/modulardiffusion-design/Modular_diffusion`. The study uses public benchmarks only and has no foreseeable negative societal impact, though safe and fair deployment should be considered.

A Algorithmic Details

A.1 GFDT Algorithmic Details

The entire training and inference process of GFDT is shown in Fig.5, as well as the algorithm1.

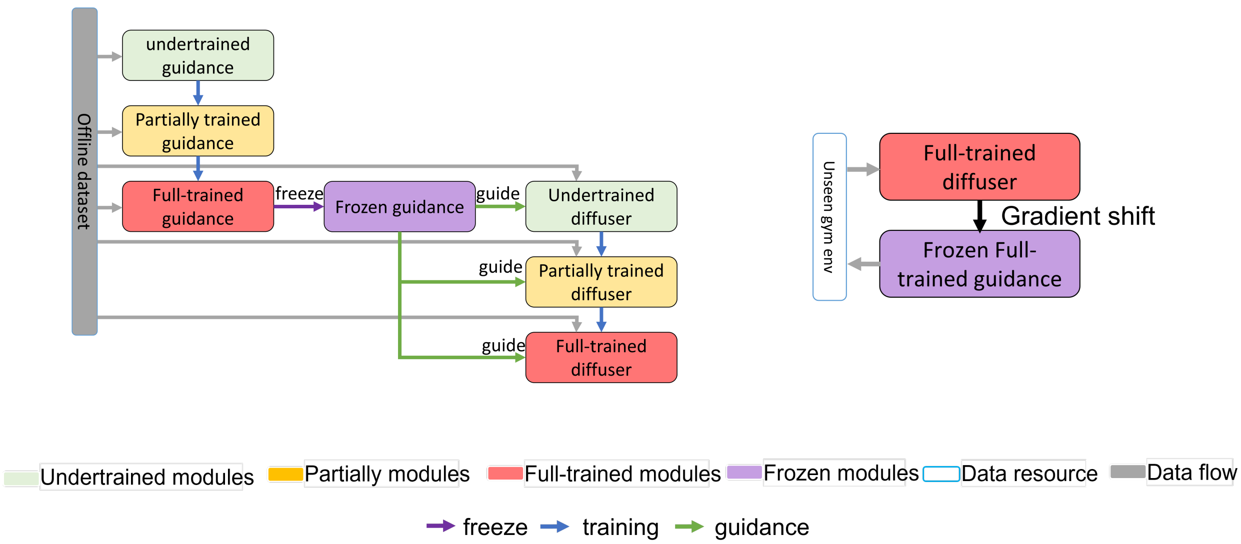

Figure 5: Training and inference stage of GFDT

Important explanation of the frozen Q network still updating the diffusion network The details of GFDT have been thoroughly explained in the main content. A reasonable concern is the role of Q_ϕ. Although Q_ϕ is frozen and does not update the parameters of the guidance network, its output values are still used to adjust the parameters of the diffusion network, encouraging it to generate samples with higher Q values.

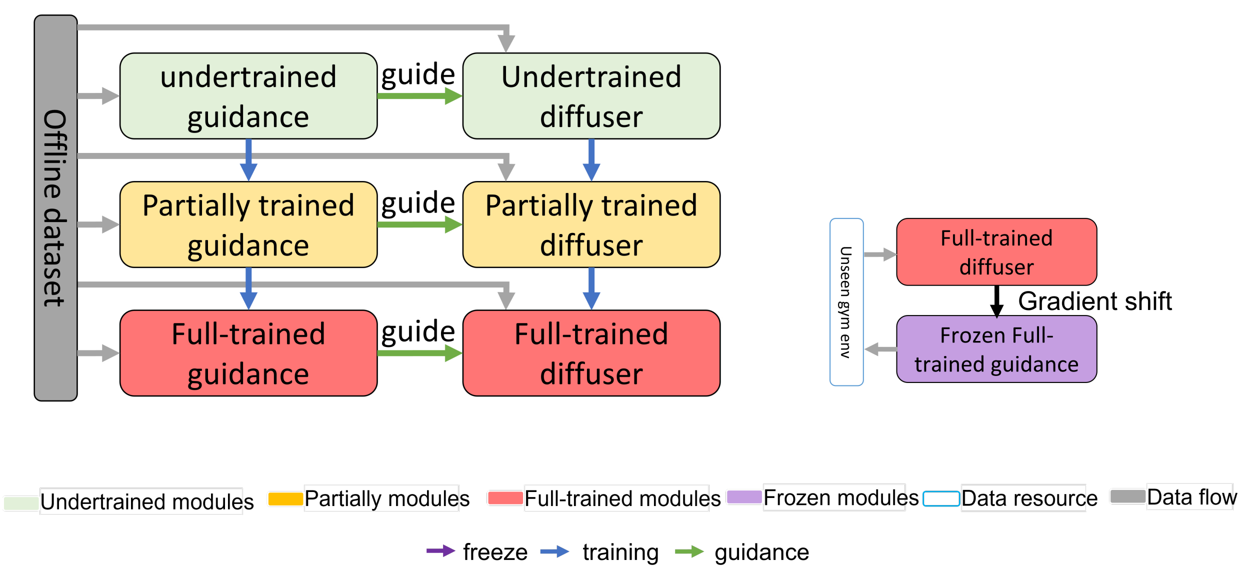

Figure 6: Training and inference stage of traditional CFG

Algorithm 2 Traditional Gradient Guidance Training

Require: Offline dataset $\mathcal{D} = \{(s, a, r, s')\}$, diffusion model ϵ_θ, Q-function Q_ϕ (learned jointly), training steps N_θ

for $j = 1$ to N_θ **do**
  Sample $(s, a_0, r, s') \sim \mathcal{D}$
  TD target: $y \leftarrow r + \gamma \cdot \max_{a'} Q_\phi(s', a')$
  Update Q_ϕ to minimize $\mathcal{L}_Q = \|Q_\phi(s, a_0) - y\|^2$
  Add noise: $a_t \leftarrow \sqrt{\bar{\alpha}_t}\, a_0 + \sqrt{1 - \bar{\alpha}_t} \cdot \epsilon, \quad \epsilon \sim \mathcal{N}(0, I)$
  Predict noise: $\hat{\epsilon} \leftarrow \epsilon_\theta(a_t, s, t)$
  Update ϵ_θ to minimize $\mathcal{L}_{\text{diff}} = \|\hat{\epsilon} - \epsilon\|^2 + \mathcal{L}_Q$
Return trained ϵ_θ, jointly-trained Q_ϕ

Inference:
for denoise steps **do**
  Sample candidate $a_k \sim \pi_\theta(\cdot|s)$
  Apply guidance: $a_{k-1} \leftarrow a_k + \lambda \cdot \nabla_a Q_\phi(s, a_k)$
Return $a^\star$

A.2 IDQL Algorithmic Details

Training. Implicit Diffusion Q-learning (IDQL) decouples the training of the diffusion model from the Q-value estimator. The diffusion policy $\pi_\theta(a|s)$ is trained purely by behavior cloning (BC) from the offline dataset $\mathcal{D} = \{(s, a)\}$, i.e.,

$$\min_\theta \ \mathbb{E}_{(s,a)\sim\mathcal{D}} \left[\|a - \pi_\theta(s)\|^2\right], \tag{11}$$

without any reward or Q-guidance incorporated into the diffusion process. In parallel, a separate Q-network $Q_\phi(s, a)$ is learned by standard temporal-difference (TD) regression:

$$\min_\phi \ \mathbb{E}_{(s,a,r,s')\sim\mathcal{D}} \left[\Big(Q_\phi(s, a) - (r + \gamma \max_{a'} Q_\phi(s', a'))\Big)^2\right]. \tag{12}$$

Notably, the Q-network is updated together with the diffusion model during training, although it does not directly affect the diffusion optimization.

Inference. At deployment, the diffusion model generates n candidate actions $\{a_1, a_2, \ldots, a_n\}$ sampled from the diffusion model $\pi_\theta(\cdot|s)$. These are then evaluated with the learned Q-network, and the action with the highest Q-value is selected:

$$a^\star = \arg\max_{i=1,\ldots,K} Q_\phi(s, a_i). \tag{13}$$

This procedure can also be interpreted as a one-hot selection mechanism over the candidate actions, where the Q-network acts as a ranking function. The algorithm of IDQL is in

Comparison between GFDT and IDQL The key distinction between IDQL and our proposed GFDT lies in how Q-guidance is incorporated. In IDQL, a separate Q-guidance network is trained, but reward information is not injected into the diffusion model during training. This design makes IDQL relatively stable under the distribution, since the learned policy is not directly biased by Q-values that could otherwise push the distribution toward out-of-distribution regions. However, the downside is that the policy is less reward-optimal, because it is guided primarily by behavioral cloning rather than directly exploiting reward signals. At inference time, IDQL applies reward guidance only as a one-hot selection among the generated actions. While this procedure ensures the selected actions are rewarding, they remain restricted to the support of the behaviorally cloned generator, which limits the achievable performance compared to gradient-guided methods.

In contrast, GFDT explicitly integrates Q-guidance into the generative diffusion process. Reward information actively shapes the learned distribution during training, which leads to more reward-aligned behaviors. At inference time, GFDT further applies a gradient shift, using gradient descent to nudge the generated

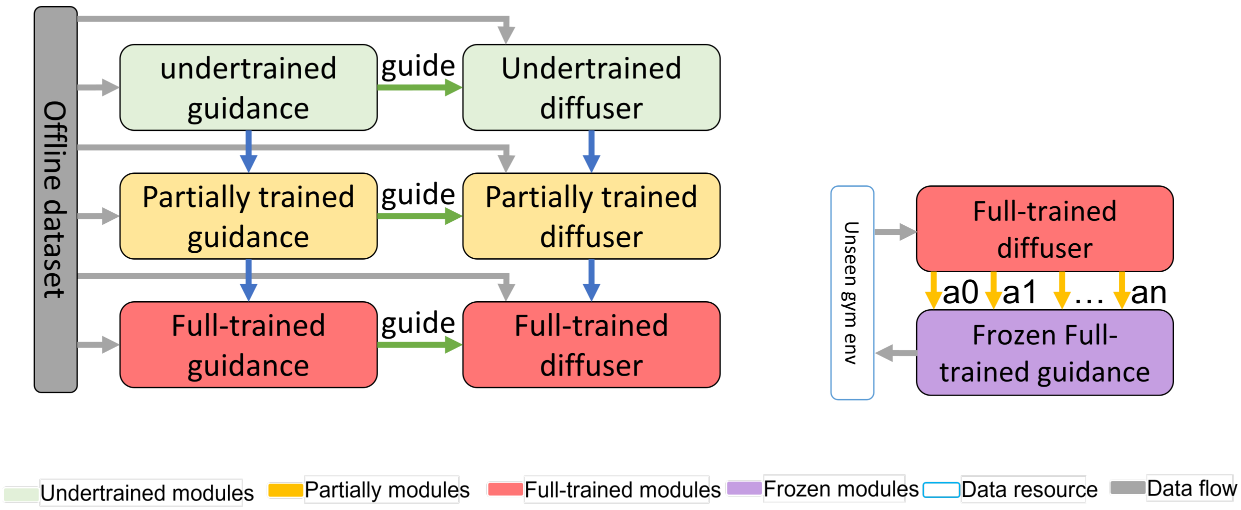

Figure 7: Training and inference stage of traditional CFG.

Algorithm 3 Implicit Diffusion Q-learning (IDQL)

Input: offline dataset $\mathcal{D}$
Initialize diffusion policy π_θ and Q-network Q_ϕ
while not converged **do**
    Sample batch (s, a, r, s') from $\mathcal{D}$
    Update π_θ by behavior cloning on (s, a)
    Update Q_ϕ by TD regression on (s, a, r, s')

Inference:
Input: state s
for $k = K, K-1, \ldots, 1$ **do**
    for $n = 1, \ldots, N$ **do**
        Sample candidate action $a_n^{(k)} \sim \pi_\theta(\cdot \mid s)$
        Evaluate $Q_\phi(s, a_n^{(k)})$
    Select best action at step k:

$$a^{(k)\star} = \arg\max_{n=1,\ldots,N} Q_\phi(s, a_n^{(k)})$$

Return $a^{(1)\star}$

---

action toward the locally optimal point. As a result, GFDT consistently outperforms both the baseline CFG and IDQL in experiments. Although gradient-based guidance has the potential to destabilize training, normalization and a staged training scheme mitigate this risk: reconstruction dominates in the early phase and Q-guidance gradually takes effect afterwards, and therefore, destabilized training can manifest a certain V-shape mode. (see Appendix G).

B Trajectory-based Guidance: Why it Fails in Offline RL

This algorithm currently does not apply to trajectory-based methods. We trained several trajectory-return guided variants; however, the guidance estimates did not *converge* in the actionable sense: they moved from near-zero to a coarse range (e.g., $200-300$ in a median expert dataset with Q values of $\approx 200-300$) but could not refine within that band, making the guidance ineffective. If the guidance itself is not converged, our method also does not make a difference. We attribute this to (i) noisy returns and (ii) long-horizon credit assignment, both exacerbated in offline settings without on-policy rollouts. By contrast, TD-based (s, a)-level guidance provides stable, local gradients that are compatible with diffusion updates.

C Experimental Setup and Hyperparameters

.All models are trained using the D4RLMuJoCoTD Dataset (Fu et al., 2021). It provides pre-collected trajectories of varying quality, including expert, medium-expert, medium-replay, and medium datasets, enabling rigorous training of offline RL algorithms under diverse data distributions. The evaluation is done in randomly initialized environments. All the gradient steps mentioned are with respect to a batch size of 256.

Wherever possible, we adopt the original hyperparameter settings from the paper of (Wang et al., 2024). Intentionally, we do not modify any training-related components—including the optimizer, learning rate, batch size, architecture, or loss function. Because a key strength of our method is that it achieves superior performance without requiring any changes to the other parameters other than pretraining or modularize. This highlights the robustness and plug-and-play nature of our approach. Final results are reported, averaged over 50 evaluation episodes. Performance is measured by normalized return, and we report both the mean(Section 4.1)).

All experiments were implemented in PyTorch and based on the CleanDiffuser framework (Wang et al., 2024). We strictly followed the hyperparameter settings from the baseline implementations to ensure fair comparison. Table 9 summarizes the key values.

Table 9: Hyperparameters used in our experiments (inherited from CleanDiffuser).

Parameter	Value	Notes
Optimizer	Adam	
Learning Rate	3×10^{-4}	fixed across all models
Batch Size	256	
Discount Factor γ	0.99	
Noise Schedule	cosine	unless otherwise specified
Number of Diffusion Steps T	5,10,20,30,40	
Actor Loss Weight η	1.0	scales $\mathcal{L}_Q$

For reproducibility, we will release full training scripts and environment configurations in our code repository.

D Why the generated action with the GFDT and the modular methods are in distribution

Addressing a Key Concern One might naturally worry that even if the guidance module (e.g., the Q-function Q_ϕ) and the diffusion model are both trained solely on the offline dataset $\mathcal{B}$, their combination during sampling could still produce out-of-distribution actions. The value guidance term $\nabla_a Q_\phi(a)$ may have a large magnitude or steep gradients, which could push the sampled action a_t away from the data manifold if not properly controlled. Therefore, the perturbation magnitude and the guidance magnitude are tightly controlled, and the guidance gradient is normalized :

$$\|a_{t+1} - a_t\| \leq \lambda + \mathcal{O}(\sqrt{\tau_t}), \lambda > 0 \ and \ \lambda \to 0$$

ensuring that each sampling step stays within a small neighborhood of the current point. Since the diffusion model is trained on the dataset $\mathcal{B}$ and generates samples close to it, and since the guidance is applied as a *soft* correction, the overall sampling trajectory remains near the support of $\mathcal{B}$. Thus, even when guided by Q_ϕ, the diffusion process remains effectively batch-constrained.

E Comparison Table of GFDT

This section contains two performance comparison tables Table.10 and Table. 11, that shows the percentages of improvement of GDFT and as other methods, compared to baseline models.

Table 10: Mujoco and Antmaze results of DQL. Each cell shows the raw score and the relative performance (%).

Environment	Baseline	GFDT	GFDT(%)	GAI	GAI(%)	BC	BC(%)	Unfreeze(%)
halfcheetah-expert	88.21	90.43	102.51%	68.49	77.65%	85.82	97.29%	101.47%
halfcheetah-medium-expert	88.28	90.18	102.15%	89.73	101.64%	85.53	96.88%	101.67%
halfcheetah-medium-replay	67.38	67.93	100.81%	67.76	100.57%	55.87	82.92%	100.08%
halfcheetah-medium	59.88	66.99	111.88%	53.36	89.12%	54.57	91.13%	91.93%
hopper-expert	166.76	172.90	103.68%	162.68	97.55%	165.11	99.01%	93.03%
hopper-medium-expert	168.00	172.31	102.56%	166.28	98.98%	166.88	99.33%	94.70%
hopper-medium-replay	151.59	152.98	100.91%	121.97	80.46%	113.30	74.74%	99.28%
hopper-medium	143.92	147.06	102.18%	71.09	49.40%	118.08	82.04%	100.47%
walker2d-expert	117.25	120.25	102.56%	119.91	102.28%	108.05	92.16%	100.57%
walker2d-medium-expert	117.73	117.63	99.91%	115.08	97.75%	117.45	99.76%	100.65%
walker2d-medium-replay	92.96	95.62	102.86%	80.32	86.40%	87.14	93.74%	102.86%
walker2d-medium	87.65	87.89	100.27%	77.33	88.22%	82.28	93.87%	100.27%
Average	112.47	115.18	102.69%	99.50	89.17%	103.34	91.91%	98.91%
antmaze-large-diverse-v2	63.33	90.67	143.16%	86.67	136.84%	66.00	104.21%	136.84%
antmaze-large-play-v2	90.00	89.33	99.26%	88.67	98.52%	50.67	56.30%	101.48%
antmaze-medium-diverse-v2	93.33	97.33	104.29%	94.00	100.71%	78.00	83.57%	102.86%
antmaze-medium-play-v2	67.33	91.33	135.64%	88.67	131.68%	68.00	100.99%	138.61%
Average	78.50	92.17	120.59%	89.50	116.94%	65.67	86.27%	119.95%

Table 11: Mujoco and Antmaze results of EDP. Each cell shows the raw score and the relative performance (%).

Environment	EDP_baseline	GFDT	GFDT(%)	GAI	GAI(%)	BC	BC(%)	Unfreeze(%)
halfcheetah-expert	86.55	86.82	100.30%	78.78	91.02%	85.82	99.15%	99.34%
halfcheetah-medium-expert	86.74	87.16	100.48%	78.18	90.14%	85.53	98.61%	100.12%
halfcheetah-medium-replay	65.78	64.42	97.94%	47.08	71.57%	55.87	84.94%	97.94%
halfcheetah-medium	54.59	59.26	108.57%	53.56	98.12%	54.57	99.96%	101.36%
hopper-expert	161.23	163.65	101.50%	151.93	94.23%	165.11	102.41%	100.63%
hopper-medium-expert	161.36	163.95	101.61%	141.07	87.43%	166.88	103.42%	101.44%
hopper-medium-replay	112.16	139.75	124.60%	114.32	101.93%	113.30	101.02%	106.91%
hopper-medium	141.16	141.64	100.35%	83.25	58.98%	118.08	83.65%	100.27%
walker2d-expert	116.14	116.34	100.18%	114.27	98.39%	108.05	93.04%	100.19%
walker2d-medium-expert	116.31	116.59	100.24%	109.55	94.19%	117.45	100.98%	100.65%
walker2d-medium-replay	85.02	83.77	98.53%	68.84	80.97%	87.14	102.49%	100.19%
walker2d-medium	84.24	84.21	99.96%	58.21	69.10%	82.28	97.67%	100.24%
Average	105.94	108.96	102.86%	91.59	86.34%	103.34	97.28%	100.77%
antmaze-large-diverse-v2	30.67	34.67	113.05%	28.67	93.48%	10.67	34.78%	154.35%
antmaze-large-play-v2	21.33	22.67	106.25%	18.67	87.50%	18.67	87.50%	118.75%
antmaze-medium-diverse-v2	67.33	52.00	77.23%	2.00	2.97%	18.00	26.73%	19.80%
antmaze-medium-play-v2	73.30	118.00	160.98%	90.00	122.78%	76.00	103.68%	154.62%
Average	48.16	56.83	114.38%	34.83	76.68%	30.83	63.17%	111.88%

F Detailed Analysis of Plug-and-play

	DGID: DGID (DQL-Guidance + IDQL-Diffusion): DGID follows the overall pipeline of IDQL, meaning that its generation and diffusion process are still driven by IDQL's methodology. The key difference is that the component responsible for selecting optimal action candidates has been replaced by a DQL module.	**IGDD: IGDD (IDQL-Guidance + DQL-Diffusion):** IGDD is built upon DQL's architecture and training logic, but replaces its gradient-based optimization module with the advantage-guided update mechanism from IDQL.
MUJOCO Environment Characteristics: MuJoCo's dense-reward nature provides immediate evaluative feedback at every timestep. This continuous supervision allows the agent to quickly identify and correct suboptimal actions, effectively smoothing the learning curve. Consequently, the environment is forgiving to small deviations or approximation errors, as incorrect behaviors are rapidly penalized and adjusted.	Compared to the original IDQL, DGID achieves a significant performance improvement, with an average score of 112.75, and becomes competitive with the baseline DQL model. The DQL module offers a strong optimization signal that effectively give IDQL a most deterministically optimal guidance on the action choice, during inference. Since the MuJoCo environment provides dense and continuous rewards, the system can directly benefit from DQL's precise action evaluation. The dense-reward setting also makes the model more tolerant to small distribution mismatches between DQL and IDQL(errors corrected immediately), leading to stable and superior overall performance.	This effectively smooths the optimization trajectory and regularizes the learning process. IGDD performs slightly better than the original DQL, achieving an average score of 115.97 and showing improved stability during diffusion. The IDQL-style advantage guidance provides smoother gradients and prevents overly aggressive Q-value maximization, which is a known issue in pure DQL setups. The result is a more balanced and robust optimization process that preserves DQL's iterative refinement strength while improving convergence reliability. In dense-reward environments like MuJoCo, where feedback is immediate and continuous, this regularized update leads to steady and consistent performance gains.
antmaze: the task follows a typical sparse-reward setting, where the agent only receives a positive signal upon successful completion of the maze. Due to the extremely long horizons—often spanning thousands of steps—the model requires high precision and the accumulated errors are not easily corrected. Moreover, the environment is heavily affected by noise and stochastic dynamics, making it highly sensitive to approximation errors.	It is suspected that When the DQL guidance is applied to out-of-distribution actions generated by IDQL, which does not generate the most rewarding signal every step, its Q-values become unreliable and often misleadingly high.(recall that mujoco is less noisy and easy to correct errors). The sharp, deterministic MaxQ operator further amplifies these estimation errors, leading to unstable and degraded performance. The main reason for the lower performance of PAP is antmaze needs conservative high precision and the broken of assumption of "small enough steps and long enough trajectory" became several in this sensitive environment.	(DGID follows IDQL's pipeline, but replaces its action selection with DQL's MaxQ-guided module). IGDD achieves a suboptimal result in AntMaze, with an average score of 62.17. It underperforms relative to original DQL but remains noticeably better than DGID. Because the IDQL-style guidance provides weaker but smoother signals, it is insufficient for the sparse-reward nature of AntMaze. This environment only provides a final success reward, so precise long-horizon navigation depends on sharp gradient signals to correctly guide early steps. The lack of strong feedback causes gradual error accumulation across iterations, leading to less efficient exploration and reduced success rates.

G Details of Application Scope

These are all the plots of cross experiments. We did not perform data mixing experiments because, as shown in the study by Miao et al. (2023), mixing datasets Generated from different policies can lead to degraded performance. Our ablation on the OOD dataset does not involve dataset mixing, since the diffusion model and the guidance model are each trained on only one dataset. Consequently, the diffusion model does not learn from multiple policies. However, when the guidance model is trained on a different dataset, it may fail to provide correct gradient signals.

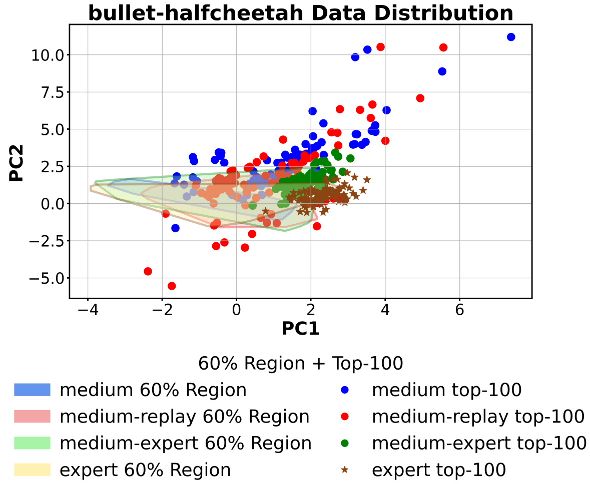

(a) density hulls (top 100, $k = 20$) of Half Cheetah

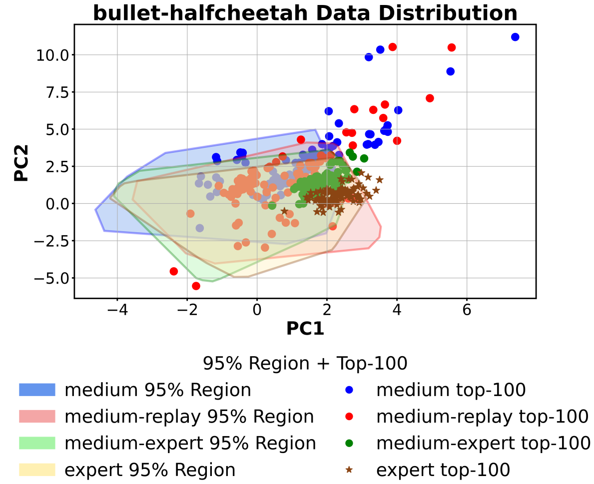

(b) PCA hull and top 100 samples of Half Cheetah

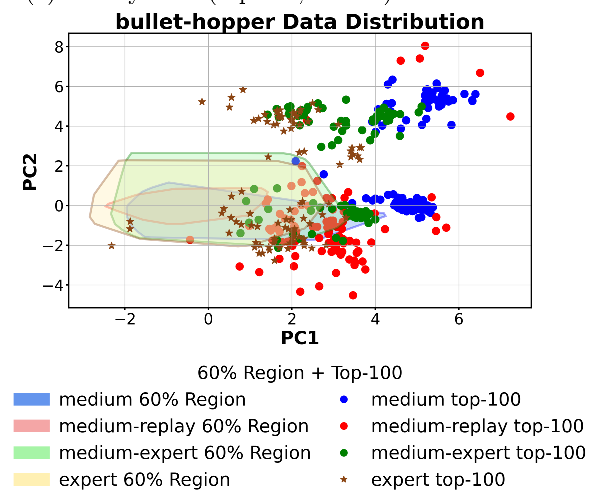

(a) density hulls (top 100, $k = 20$) of Hopper

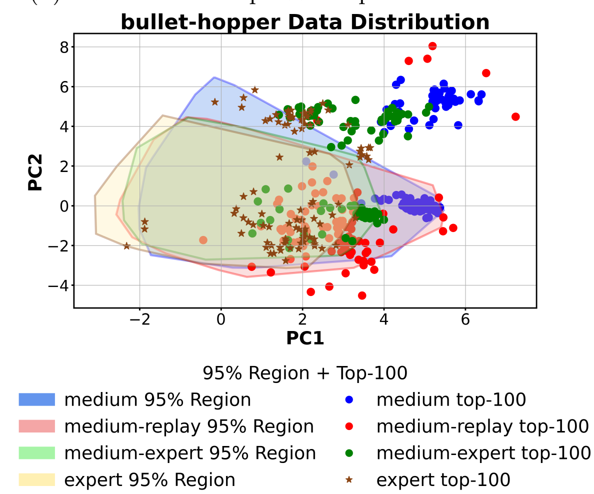

(b) PCA hull and top 100 samples of hopper

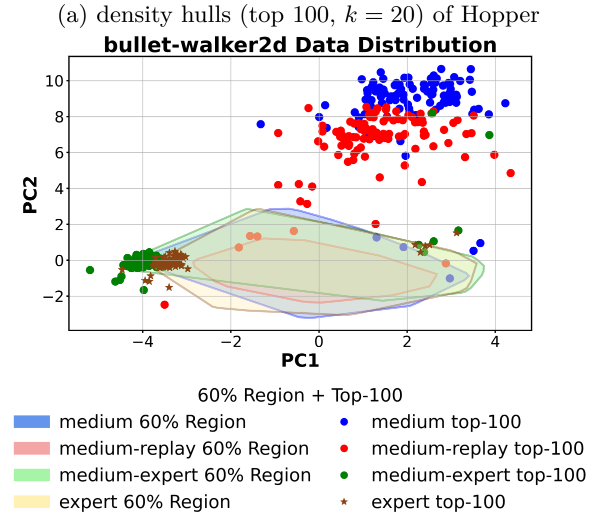

(a) density hulls (top 100, $k = 20$) of Walker2d

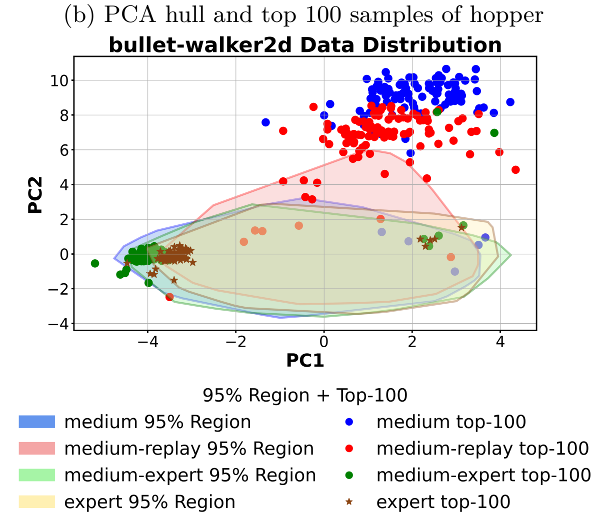

(b) PCA hull and top 100 samples of Walker2d

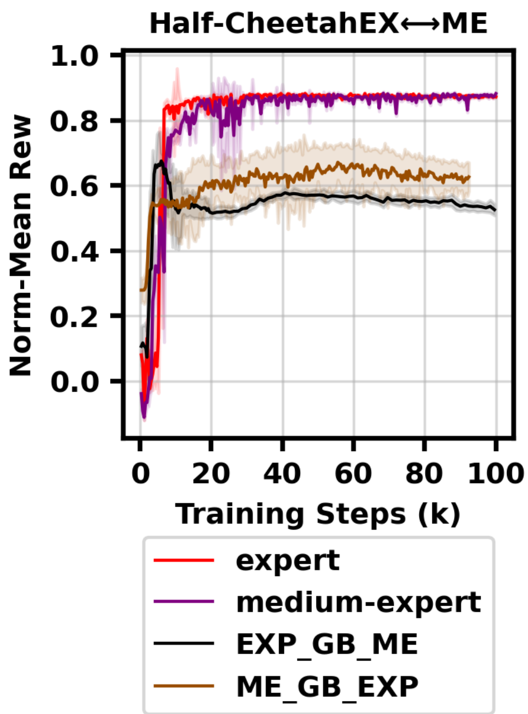

(a) Across Experiments of Expert (EX) and Medium Expert (ME)

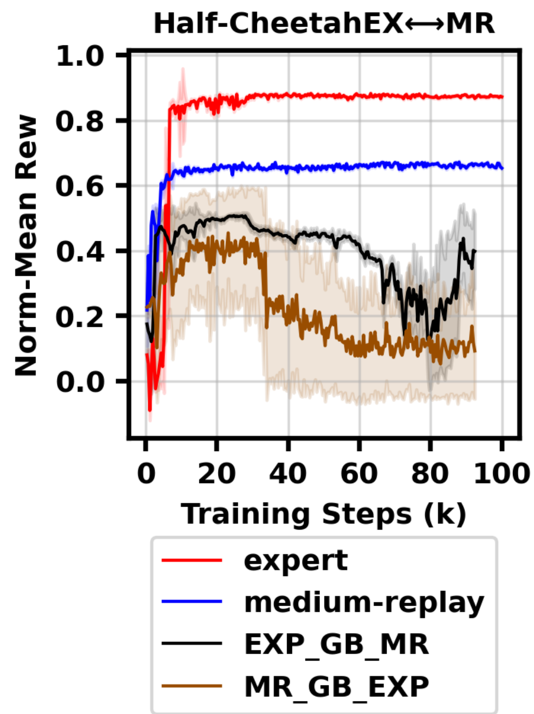

(b) Across Experiments of Expert(EX) and Medium Replay(MR)

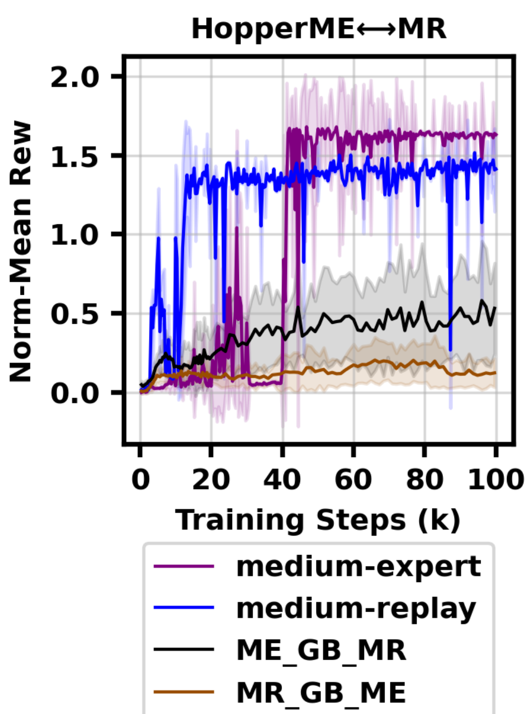

(c) Across Experiments of Medium Expert(ME) and Medium Replay(MR)

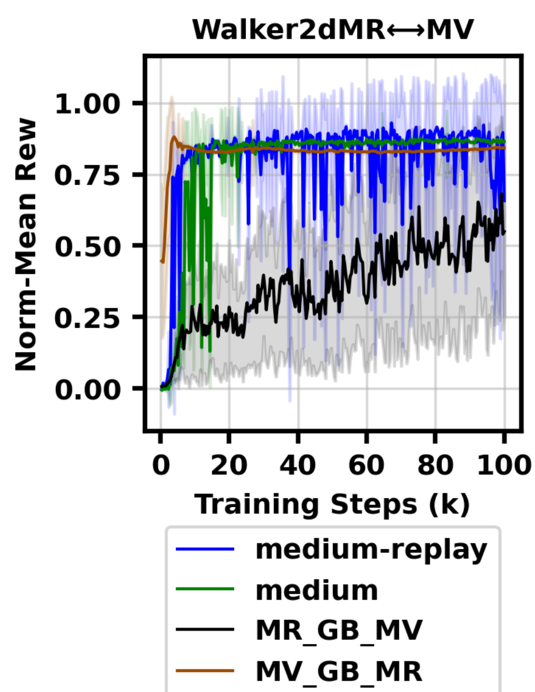

(d) Across Experiments of Medium Replay(MR) and Medium(MV)

H Notation and Terminology

Symbol	**Meaning**
$\mathcal{D}$	Offline dataset consisting of tuples (s, a, r, s'), collected by an unknown behavior policy and fixed throughout training.
s, a, r, s'	State, action, reward, and next state sampled from the offline dataset $\mathcal{D}$.
π_θ	Diffusion-based policy parameterized by θ. The policy is defined implicitly by a conditional reverse diffusion process, not by an explicit density.
θ	Parameters of the diffusion (denoising) network that generates actions.
a_0	Clean (final) action generated by the diffusion policy or taken from the dataset.
a_t	Noisy action at diffusion timestep t.
ϵ_θ	Denoising network used in the diffusion policy, trained to predict the injected noise during diffusion.
$Q(s, a)$	state–action value function, defined as the expected discounted return starting from (s, a).
Q_θ	Parameterized guidance module (Q-network) trained on the offline dataset using temporal-difference learning. It serves as a different reward estimator from and provides gradient-based guidance to the diffusion model.
ϕ	Parameters of the guidance module Q_ϕ.
Q_ϕ	A **pretrained and frozen** guidance module. This Q-network is trained independently (e.g., via DQL or IDQL) and reused to guide diffusion training or inference without further updates.
$\tilde{Q}_\phi$	Normalized Q-value used for guidance, obtained by rescaling $Q_\phi(s, a)$ to ensure scale invariance across different algorithms and modules.
$\nabla_a Q_\phi$	Gradient of the guidance module with respect to the action, used to bias diffusion sampling toward higher-value actions.

Table 12: Symbol definitions and meanings

Table 13: Algorithm Abbreviations

Abbreviation	Explanation
Env	**Environment.** The benchmark task or environment in which the algorithm is evaluated (e.g., HalfCheetah, Hopper, Walker2d, AntMaze).
ReBR	**Regularized Behavior Regularized Actor Critic (ReBRAC).** A conservative offline RL algorithm emphasizing stability through behavior regularization (Wu et al., 2019).
DICE	**Dynamic Importance Sampling Correction Estimator.** An offline RL method that uses importance weighting to correct distribution mismatch during policy evaluation (Ma et al., 2024).
CQL	**Conservative Q-Learning.** A value-based offline RL algorithm that penalizes overestimation of unseen actions to ensure conservative value estimation (Kumar et al., 2020).
IQL	**Implicit Q-Learning.** A decoupled offline RL method that learns Q-values and implicitly defines a policy via advantage-weighted regression without explicit policy optimization (Kostrikov et al., 2022).
DQL_GF	**Diffusion Q-Learning with Guidance-First (GFDT).** The DQL algorithm trained under the Guidance-First Diffusion Training paradigm, where the Q-network is pretrained and frozen before diffusion training.
EDP_GF	**Efficient Diffusion Policy with Guidance-First (GFDT).** A one-step denoising diffusion policy algorithm enhanced with pretrained frozen guidance to accelerate convergence and improve efficiency.
GFDT	**Guidance-First Diffusion Training.** A training paradigm where the guidance (Q-network) is pretrained and frozen before training the diffusion policy.
Baseline	The original implementation of the corresponding diffusion-based offline RL algorithm (e.g., DQL, IDQL, or EDP) without our proposed modifications.
D-Baseline	**Double-Guidance Baseline.** A variant of the baseline model where the guidance module used during inference is replaced with an independently initialized version of the same architecture (different random seed).
Double_GFDT	GFDT equipped with *Double Guidance* at inference time, reducing variance through independent initialization.
GAI	**Guidance at Inference.** A behavior cloning model trained without reward guidance during training, but augmented with Q-guidance only at inference.
Unfreeze	A variant of GFDT where the pretrained guidance module is not frozen but continues to be updated during policy training.
BC	**Behavior Cloning.** A supervised learning baseline that trains a policy to imitate dataset actions without reward guidance.
DGID	**DQL-Guidance with IDQL-Diffusion.** A plug-and-play configuration where the **guidance module** is taken from DQL (D), while the **diffusion policy** is taken from IDQL (I). Here, D denotes DQL, I denotes IDQL, G denotes the guidance module, and the final D denotes the diffusion model.
IGDD	**IDQL-Guidance with DQL-Diffusion.** A plug-and-play configuration where the **guidance module** is taken from IDQL (I), while the **diffusion policy** is taken from DQL (D). The notation follows the same convention: I/D indicate the algorithm source (IDQL or DQL), G denotes the guidance module, and D denotes the diffusion model.

Table 14: D4RL Benchmark Environment Abbreviations

Abbreviation	**Explanation**
HCEX	**HalfCheetah-Expert.** Dataset generated by an expert policy in the HalfCheetah environment.
HCME	**HalfCheetah-Medium-Expert.** Dataset generated by a mixture of medium and expert policies in HalfCheetah.
HCMR	**HalfCheetah-Medium-Replay.** Dataset generated by replay buffer data collected from medium-performance policies.
HCMV	**HalfCheetah-Medium.** Dataset generated by a medium-performance policy in HalfCheetah.
HOEX	**Hopper-Expert.** Dataset generated by an expert policy in the Hopper environment.
HOME	**Hopper-Medium-Expert.** Dataset generated by a mixture of medium and expert policies in Hopper.
HOMR	**Hopper-Medium-Replay.** Replay buffer dataset in Hopper.
HOMV	**Hopper-Medium.** Dataset generated by a medium policy in Hopper.
WAEX	**Walker2d-Expert.** Expert policy dataset in Walker2d.
WAME	**Walker2d-Medium-Expert.** Mixed dataset in Walker2d.
WAMR	**Walker2d-Medium-Replay.** Replay dataset in Walker2d.
WAMV	**Walker2d-Medium.** Medium policy dataset in Walker2d.

I Error bound calculation with respect to gradient steps

In this appendix, we provide a simple scaling calculation to clarify how the number of training steps depends on the desired relative error reduction. This calculation is intended purely for intuition and does not constitute a formal convergence guarantee.

We start from a generic estimation bound of the form

$$\mathbb{E}\big[\|\nabla_a Q_\phi - \nabla_a Q^*\|\big] \;\le\; C\left(\frac{L}{\sqrt{N}} + \epsilon\right), \tag{14}$$

where C is a constant depending on the function class, L is a Lipschitz-related constant ensuring continuity, N denotes the number of training steps (or effective samples), and ϵ captures lower-order optimization or approximation error.

Ignoring ϵ. In practice, ϵ is typically much smaller than the dominant statistical term once optimization has progressed, and is therefore neglected in the following back-of-the-envelope calculation.

Reference error level. When $N = 1$, the bound reduces to

$$\mathbb{E}\big[\|\nabla_a Q_\phi - \nabla_a Q^*\|\big] \;\le\; CL, \tag{15}$$

which corresponds to an untrained or randomly initialized network. We take this quantity as a reference level, corresponding to a 100% relative error under a normalized scale.

Relative error reduction. Suppose we aim to reduce the error to a fraction $\delta \in (0, 1)$ of its initial level.

$$\mathbb{E}\big[\|\nabla_a Q_\phi - \nabla_a Q^*\|\big] \;\le\; \delta\, CL. \tag{16}$$

Substituting the bound and canceling the shared constants C and L (which are fixed for the same network and function class) yields

$$\frac{CL}{\sqrt{N}} \;\le\; \delta CL. \tag{17}$$

Solving for N gives

$$N \;\ge\; \frac{1}{\delta^2}. \tag{18}$$

Examples. For a 1% relative error ($\delta = 0.01$), this requires $N \ge 10^4$ training steps. For a 10% relative error ($\delta = 0.1$), this requires $N \ge 10^2$ training steps. The same calculation applies to an error requirement of 0.1%.This illustrates that even modest relative accuracy targets can correspond to large differences in training cost.

Discussion. This calculation depends on the relative error reduction under fixed function-class constants. Since the quantity under consideration is already normalized to lie in $[0, 1]$, a 1% error directly corresponds to a 1% relative deviation under this normalized scale. This is exactly the same notion of relative error used in the preceding discussion. The specific values of C and L are not critical, as they cancel when comparing different accuracy levels for the same network. The purpose of this appendix is solely to provide an order-of-magnitude intuition for computational savings, rather than a task- or environment-specific error interpretation.

References

Anurag Ajay, Yilun Du, Abhi Gupta, Joshua B. Tenenbaum, Tommi S. Jaakkola, and Pulkit Agrawal. Is conditional generative modeling all you need for decision making? In *International Conference on Learning Representations*, 2023. Top 5% of submissions.

Jacob Andreas, Dan Klein, and Sergey Levine. Modular multitask reinforcement learning with policy sketches. In *International Conference on Machine Learning*, 2017. URL `https://arxiv.org/abs/1704.06643`.

Hyungjin Chung, Byungsoo Sim, and Jong Chul Ye. Diffusion posterior sampling for general noisy inverse problems. *International Conference on Learning Representations*, 2023.

Prafulla Dhariwal and Alex Nichol. Diffusion models beat gans on image synthesis. In *Advances in Neural Information Processing Systems*, 2021.

Arnaud Doucet, Nando de Freitas, and Neil Gordon. *Sequential Monte Carlo Methods in Practice*. Springer, 2009.

The Farama Foundation. Gymnasium: A standard api for reinforcement learning environments. https://github.com/Farama-Foundation/Gymnasium, 2024.

Justin Fu, Aviral Kumar, Ofir Nachum, George Tucker, and Sergey Levine. D4rl: Datasets for deep data-driven reinforcement learning. In *Advances in Neural Information Processing Systems Datasets and Benchmarks Track*, 2021. URL `https://datasets-benchmarks-proceedings.neurips.cc/paper/2021/file/7b5b23f4aadf9513306bcd59afb6e4c9-Paper-round2.pdf`.

Scott Fujimoto, Edoardo Conti, Mohammad Ghavamzadeh, and Joelle Pineau. Benchmarking batch deep reinforcement learning algorithms. *arXiv preprint arXiv:1910.01708*, 2019a.

Scott Fujimoto, David Meger, and Doina Precup. Off-policy deep reinforcement learning without exploration. In *International Conference on Machine Learning*, pp. 2052–2062, 2019b.

Kelvin Guu, Kenton Lee, Zora Tung, Panupong Pasupat, and Ming-Wei Chang. Realm: Retrieval-augmented language model pre-training. In *International Conference on Machine Learning*, pp. 3929–3938, 2020.

Philippe Hansen-Estruch, Ilya Kostrikov, Michael Janner, Jakub Grudzien Kuba, and Sergey Levine. Idql: Implicit q-learning as an actor-critic method with diffusion policies. *arXiv preprint arXiv:2304.10573*, 2023.

Jonathan Ho and Tim Salimans. Classifier-free diffusion guidance. *arXiv preprint arXiv:2207.12598*, 2022.

Jonathan Ho, Ajay Jain, and Pieter Abbeel. Denoising diffusion probabilistic models. In *Advances in Neural Information Processing Systems*, volume 33, pp. 6840–6851, 2020.

Gautier Izacard and Edouard Grave. Leveraging passage retrieval with generative models for open domain question answering. In *Conference on Empirical Methods in Natural Language Processing*, pp. 8741–8754, 2021.

Gautier Izacard, Edouard Grave, Fabio Petroni, Lucas Hosseini, Timo Schick, Pierre-Emmanuel Mazare, Julian Eisenschlos, Sebastian Petrov, Vladimir Karpukhin, Patrick Lewis, Wen-tau Yih, Tim Rocktaschel, Sebastian Riedel, and Douwe Kiela. Atlas: Few-shot learning with retrieval augmented language models. In *International Conference on Machine Learning*, 2022.

Michael Janner, Yilun Du, Joshua B. Tenenbaum, and Sergey Levine. Planning with diffusion for flexible behavior synthesis. In *International Conference on Machine Learning*, 2022. URL `https://arxiv.org/abs/2205.09991`.

Bingyi Kang, Haotian Shi, Yilun Tan, Mingming Zhu, Dahuan Lin, and Hang Zhou. Efficient diffusion policies for offline reinforcement learning. *arXiv preprint arXiv:2310.03573*, 2023.

Dongjun Kim, Yeongmin Kim, Se Jung Kwon, Wanmo Kang, and Il-Chul Moon. Refining generative process with discriminator guidance in score-based diffusion models. In *International Conference on Machine Learning*, volume 202, pp. 1–25. PMLR, 2023.

Ilya Kostrikov, Ashvin Nair, and Sergey Levine. Offline reinforcement learning with implicit q-learning. In *International Conference on Learning Representations (ICLR)*, 2022.

Aviral Kumar, Aurick Zhou, George Tucker, and Sergey Levine. Conservative q-learning for offline reinforcement learning. In *Advances in Neural Information Processing Systems*, volume 33, pp. 1179–1191, 2020.

Sergey Levine, Aviral Kumar, George Tucker, and Justin Fu. Offline reinforcement learning: Tutorial, review, and perspectives on open problems. *arXiv preprint arXiv:2005.01643*, 2020.

Patrick Lewis, Ethan Perez, Aleksandra Piktus, Fabio Petroni, Vladimir Karpukhin, Naman Goyal, Heinrich Küttler, Mike Lewis, Wen-tau Yih, Tim Rocktäschel, Sebastian Riedel, and Douwe Kiela. Retrieval-augmented generation for knowledge-intensive nlp tasks. In *Advances in Neural Information Processing Systems*, 2020.

Xinyang Li et al. Restart sampling for improving diffusion models. *arXiv preprint arXiv:2306.XXXXX*, 2023.

Cheng Lu, Shengming Ruan, Yang Song, and Stefano Ermon. Energy-based guidance for diffusion models. In *International Conference on Machine Learning*, 2023.

Xingyu Ma, Yuchen Yang, Yifei Chen, Han Liu, and Tong Zhang. Dice: Offline reinforcement learning with diffusion models. In *International Conference on Learning Representations (ICLR)*, 2024.

Xiyang Ma, Fangchen Luo, Nan Jiang, Ofir Nachum, and Dale Schuurmans. Revisiting the minimalist approach to offline reinforcement learning. In *Advances in Neural Information Processing Systems (NeurIPS)*, 2023. URL `https://proceedings.neurips.cc/paper_files/paper/2023/hash/f0e5d0b6e6bfb14d91d60a3f3e4f0c76-Abstract-Conference.html`. NeurIPS 2023 Conference Paper.

Yilun Ma et al. Scaling diffusion models at inference time. *arXiv preprint arXiv:2503.XXXXX*, 2025.

Q. Miao et al. Learning with noisy labels using collaborative sample selection. In *Advances in Neural Information Processing Systems*, 2023.

Takeru Miyato, Toshiki Kataoka, Masanori Koyama, and Yuichi Yoshida. Spectral normalization for generative adversarial networks. In *Advances in Neural Information Processing Systems*, volume 31, 2018. URL `https://proceedings.neurips.cc/paper/2018/file/1802.05957-Paper.pdf`.

Chong Mou, Yabo Zhang, Yixiao Li, et al. T2i-adapter: Learning adapters to dig out more controllable ability for text-to-image diffusion models. *arXiv preprint arXiv:2302.08453*, 2023.

Ashvin Nair, Aviral Kumar, Chelsea Finn, and Sergey Levine. Accelerating online reinforcement learning with offline datasets. In *Advances in Neural Information Processing Systems*, 2020.

Alex Nichol, Prafulla Dhariwal, Aditya Ramesh, Pranav Shyam, Pam Mishkin, Bob McGrew, Ilya Sutskever, and Mark Chen. Glide: Towards photorealistic image generation and editing with text-guided diffusion models. In *Advances in Neural Information Processing Systems*, 2021.

Xue Bin Peng, Angjoo Kanazawa, Sam Toyer, Pieter Abbeel, and Sergey Levine. Composing complex skills by learning transition policies. In *IEEE International Conference on Robotics and Automation*, 2019. URL `https://arxiv.org/abs/1906.01068`.

Aditya Ramesh, Mikhail Pavlov, Gabriel Goh, Scott Gray, Chelsea Voss, Alec Radford, Mark Chen, and Ilya Sutskever. Zero-shot text-to-image generation. In *International Conference on Machine Learning*, 2021.

Aditya Ramesh, Prafulla Dhariwal, Alex Nichol, et al. Hierarchical text-conditional image generation with clip latents. In *Proceedings of the International Conference on Machine Learning (ICML)*, 2022.

Vasilis Skreta et al. Principled correction of diffusion sampling via feynman–kac formulations. *arXiv preprint arXiv:2502.XXXXX*, 2025.

Charles J. Stone. Optimal global rates of convergence for nonparametric regression. *The Annals of Statistics*, 10(4):1040–1053, 1982. doi: 10.1214/aos/1176345969. URL `https://projecteuclid.org/journals/annals-of-statistics/volume-10/issue-4/Optimal-Global-Rates-of-Convergence-for-Nonparametric-Regression/10.1214/aos/1176345969.full`.

Masatoshi Uehara et al. A tutorial on inference-time alignment and control in diffusion models. *Transactions on Machine Learning Research*, 2025.

Hado van Hasselt. Double q-learning. In *Advances in Neural Information Processing Systems*, volume 23, pp. 2613–2621, 2010.

Hado van Hasselt, Arthur Guez, and David Silver. Deep reinforcement learning with double q-learning. *Proceedings of the AAAI Conference on Artificial Intelligence*, 30(1), 2016.

Zhendong Wang, Xinyang Zhang, Bowen Liu, et al. Cleandiffuser: Diffusion library and benchmark for decision-making. In *Advances in Neural Information Processing Systems Datasets and Benchmarks Track*, 2024. URL `https://arxiv.org/abs/2406.09509`.

Larry Wasserman. *All of Nonparametric Statistics*. Springer Science & Business Media, New York, NY, 2006. ISBN 978-0-387-25145-5. URL `https://www.stat.cmu.edu/~larry/all-of-nonpar/`.

Yifan Wu, George Tucker, and Ofir Nachum. Behavior regularized offline reinforcement learning. In *Advances in Neural Information Processing Systems*, pp. 7968–7978, 2019.

Rui Yang, Yong Lin, Li Jiang, Xiyao Wang, Shuang Li, and Shuicheng Yan. Diffusion policies for offline reinforcement learning. In *International Conference on Machine Learning (ICML)*, 2023.

Zexiang Ye, Yixiao Zhang, et al. Ip-adapter: Text-compatible image prompt adapter for text-to-image diffusion models. *arXiv preprint arXiv:2308.06721*, 2023.

Tianhe Yu, Aviral Kumar, Yevgen Chebotar, Karol Hausman, Gaurav Sukhatme, Sergey Levine, and Chelsea Finn. Mopo: Model-based offline policy optimization. In *Advances in Neural Information Processing Systems*, pp. 14129–14142, 2020.

Lvmin Zhang, Yongjie Rao, and Maneesh Agrawala. Adding conditional control to text-to-image diffusion models. In *IEEE International Conference on Computer Vision*, 2023.

Rui Zhang, Jianfeng Lu, Tianyi Luo, Zhaoran Wang, and Mengdi Zhou. Steering diffusion models with sequential monte carlo. *arXiv preprint arXiv:2405.19567*, 2024.